https://dx.doi.org/10.1016/j.conbuildmat.2018.10.065

Structural behaviour and design of chord plastification in high strength steel CHS X-joints

Xiaoyi Lan [a], Tak-Ming Chan [a,*], Ben Young [b]

[a] Dept. of Civil and Environmental Engineering, The Hong Kong Polytechnic University, Hung Hom, Hong Kong, China
[b] Dept. of Civil Engineering, The University of Hong Kong, Pokfulam Road, Hong Kong, China
*tak-ming.chan@polyu.edu.hk

Abstract: This paper aims to investigate the structural behaviour and static strength of high strength steel circular hollow section (CHS) X-joints under axial compression in the braces. Extensive numerical simulations on the CHS X-joints using S460, S700, S900 and S1100 steel were carried out. The failure mode of the CHS X-joints investigated is chord plastification. Effects of heat affected zones on the initial stiffness and static strength of the CHS X-joints are found to be relatively insignificant. Suitability of the mean strength equation adopted by the CIDECT design guide for the CHS X-joints was evaluated against results obtained from the numerical simulations in this study and experimental tests in the literature. In general, the CIDECT mean strength prediction is slightly unconservative for CHS X-joints in S460 steel and becomes increasingly unconservative with increasing steel grade. This is because the improved yield stress of high strength steel generally could not be fully utilised in the CHS X-joints mainly due to the adopted indentation limit i.e. 3% of chord diameter. The recommended ranges of chord diameter to wall thickness ratio (2γ) are $2\gamma\leq40$ for steel grades ranging from S460 to S700 and $2\gamma\leq30$ for steel grades greater than S700 and up to S1100 to allow for more effective use of high strength steel. The suggested range of brace to chord diameter ratio (β) is $0.2\leq\beta\leq1.0$ for steel grades ranging from S460 to S1100, which is the same as the current CIDECT validity range of β ratio. A mean strength equation was proposed for the CHS X-joints with 2γ and β ratios which are within the suggested ranges. The statistical analysis shows that the proposed mean strength equation can produce reasonably accurate and consistent strength prediction. The proposed mean strength equation was converted to a design strength equation for the design of high strength steel CHS X-joints.

Keywords: Chord plastification; CHS X-joint; High strength steel; Structural behaviour; Static strength; Design

1. Introduction

The popularity of high strength steel (HSS) with a nominal yield stress higher than 450 MPa, as an economical and sustainable construction material, is increasing. The application of high strength steel with high strength-to-weight ratio in tubular structures can reduce structural self-weight, construction costs and carbon footprints because of lower consumption of steel materials. Tubular joints are critical components in onshore and offshore tubular structures as failure of one or several tubular joints could lead to the collapse of entire tubular structures. Thus, it is significant to provide design guidance for tubular joints. Comprehensive design guidance for normal strength steel tubular joints is available in design codes and guides [1-7]. In contrast, design rules for HSS tubular joints remain limited. It is therefore desirable to investigate the structural behaviour and static strength of HSS tubular joints for the design of joints and thus to facilitate application of HSS tubular structures in construction industry.

Liu and Wardenier [8] conducted finite element analysis on the static strength of rectangular hollow section (RHS) gap K-joints using S460 steel. It is found that the joint strength is on average 10 to 16% lower than that of corresponding S235 joints in relative terms. Kurobane [9] carried out tests on circular hollow section (CHS) gap K-joints in S460 steel and found that the joint strength is 18% lower compared with the same joints using S235 steel. Noordhoek et al. [10] also reported similar findings that the joint efficiency of CHS gap K-joints in S460 steel is lower than that of corresponding S235 joints. These early studies exclusively on gap K-joints show that the static strength of S460 gap K-joints is lower than that of corresponding S235 joints in relative terms. In line with the research findings, EN 1993-1-8 [1] and the CIDECT design guides [2, 3] allow the use of steel grades beyond S355 and stipulate restrictive design rules. Additional reduction factors of joint strength are specified to be applied to the design strength equations of normal strength steel tubular joints for the design of all types of HSS tubular joints indiscriminately [1-3]. EN 1993-1-8 [1] prescribes a reduction factor of 0.9 for tubular joints using steel grades greater than S355 and up to S460. EN 1993-1-12 [11] further extends the limit of steel grades beyond S460 and up to S700 and imposes a reduction factor of 0.8. Likewise, the CIDECT design guides [2, 3] stipulate a reduction factor of 0.9 and specify the limitation on yield stress (f_y) to 0.8 of the ultimate stress (f_u) for tubular joints using steel grades greater than S355 and up to S460. These restrictions are imposed for tubular joints in steel grades greater than S355 due to relatively larger deformation for chord face plastification, possibly lower deformation and rotation capacity, and required sufficient connection ductility for chord punching shear and local yielding of braces [2, 3, 12].

These restrictive provisions in EN 1993-1-8 [1] and the CIDECT design guides [2, 3] partially eliminate the benefits of using higher steel grades. The suitability of such design rules for all types of HSS tubular joints remains controversial. Some recent investigations re-evaluated the design provisions. For RHS joints, Becque and Wilkinson [13] conducted tests on RHS T- and X-joints in C450 steel with a nominal yield stress of 450 MPa. Test strengths of the joints were compared with nominal strength predictions of the CIDECT design guide [2]. The nominal strengths were converted from the CIDECT design strengths by multiplying the implicit safety factors incorporated in the CIDECT design equations. The specified reduction factor and limitation on the yield stress were not applied. It is found that the test strengths exceed the CIDECT nominal strengths for the joints which failed by ductile modes of chord face plastification and chord side wall buckling, provided that the joint parameters are within the validity ranges of the CIDECT design strength equations. The test program, however, provided justification for the application of the reduction factor and limitation on yield stress for the joints which failed by less ductile modes of chord punching shear and effective width failure of braces. Mohan et al. [14, 15] conducted numerical investigations on RHS T-, X-, K- and N-joints in C450 steel and found that the numerical strengths are generally higher than the CIDECT design strengths without applying the reduction factor and limitation on yield stress. Cheng and Becque [16] proposed a design methodology for chord side wall buckling of RHS X-joints in steel grades up to C450 subjected to axial compression in the braces which can consider the effect of compressive chord preload. For CHS joints, Puthli et al. [17] conducted tests on CHS X-joints using steel grades up to S770 and numerical analysis on the reduction factors of the static strength of CHS X-joints in S460 and S690 steel compared with the same joints using S355 steel. It is noted that the effect of chord preload was not examined. It is found that the joint strengths obtained from tests are generally higher than the design strengths calculated from design equations in EN 1993-1-8 [1] without applying the reduction factors. The reduction factors of joint strength obtained from the numerical study are higher than 0.9 for CHS X-joints in S460 and larger than 0.8 for S690 joints. Lee et al. [18] carried out test and numerical investigations on CHS X-joints using steel grades up to HSA800 with a nominal yield stress of 650 MPa and without chord preload. Similar findings that the test and numerical strengths exceed the design strengths of EN 1993-1-8 [1] without using the reduction factors were reported. Lan et al. [19] compared numerical and test strengths of CHS X-joints with nominal yield stresses ranging from 650 to 1100 MPa with those calculated from mean strength equations on which design equations in EN 1993-1-8 [1] and the CIDECT design guide [3] are based. It is found that suitability of the mean strength equations for CHS X-joints using high strength steel depends on the yield stress (f_y), brace to chord diameter ratio (β), chord diameter to wall thickness ratio (2γ) and compressive chord preload ratio (n). It is noted that the parameter ranges of CHS X-joints [17-19], however, remain limited. Comprehensive assessment of the current design rules and design guidance for CHS X-joints using high strength steel are therefore needed.

An extensive finite element investigation on the structural behaviour and static strength of CHS X-joints using S460, S700, S900 and S1100 steel subjected to axial compression in the braces was conducted. Effects of heat affected zones on high strength steel CHS X-joints were examined. The mean strength equation on which the CIDECT design equation is based for CHS X-joints which fail by chord plastification was evaluated against the numerical strengths obtained in this study and test strengths reported in the literature. Design rules were proposed for CHS X-joints using steel grades ranging from S460 to S1100.

2. Finite element investigation

2.1. Finite element model

The finite element (FE) program ABAQUS [20] was employed to conduct the numerical investigation on CHS X-joints using high strength steel. Fig. 1 shows the joint configuration and notations. Lan et al. [19] developed FE models for CHS X-joints using high strength steel which were validated against the reported test results [17, 18]. The material properties measured in the tests [17, 18] were adopted. The true stress and logarithmic plastic strain converted from engineering stress and strain were employed. Only axial displacement at the end of two brace members was allowed while other degrees of freedom were constrained, and the two chord ends were free to translate and rotate. The brace loading was applied in increments by using the "Static" method in ABAQUS. The parameter (*NLGEOM) was adopted to consider the effect of geometric nonlinearity in numerical simulations. Effects of element type and weld modelling were examined. A mesh convergence study was carried out to determine suitable mesh sizes. It is found that numerical results of FE models adopting a shell element i.e. S4R (four-node quadrilateral shell element with reduced integration) which excluded weld modelling and those using solid elements (i.e. C3D8R for the brace and chord members and C3D6 for the weld) which modelled the weld are comparable. The von Mises yield criterion and isotropic hardening rule were used. The failure mode of chord plastification, load-indentation curves and static strengths of CHS X-joints obtained from the numerical analysis were compared with those in the tests [17, 18]. It is shown that the numerical predictions agree well with the test results. The static strength of CHS X-joints is determined by the peak load or the load at an indentation of 3% of chord dimeter (d) at the crown (see Fig. 1), which was originally proposed by Lu et al. [21]. If the indentation at the peak load is smaller than 3%d, then the peak load is taken as the joint strength. Otherwise, the load at the indentation of 3%d is considered to be the joint strength.

2.2. Effects of heat affected zones

The brace members are directly welded to the chord for welded CHS X-joints. A high heat input into base metals could lead to a phase transition in heat affected zones (HAZ) and thus result in changes in microstructures and corresponding material properties. Microstructures and material properties of HAZ mainly depend on the steel material, heat input, welding type and cooling time [22, 23]. Steel manufacturing techniques e.g. quenching and tempering (QT), direct quenching (DQ), and thermo-mechanical controlled processing (TMCP) are used to produce high strength steel [23]. Chemical compositions and carbon equivalent values (CEV) of high strength steel manufactured using different techniques differ which could affect the material properties of HAZ. Stroetmann et al. [22] found that the ultimate stresses (f_u) of HAZ in QT S690Q and S960Q steel and TMCP S500M steel are generally higher than those of base metals in the cooling time ranging from 1.5 to 25 seconds. However, the ultimate stresses of HAZ in TMCP S700M steel are lower than those of base metals. This is possibly due to lower level of alloying in TMCP steel compared with QT steel. Javidan et al. [23] reported that the maximum strength reduction in HAZ of TMCP steel with a measured yield stress (f_y) of 772 MPa is around 8% and that of DQ steel with a measured yield stress of 1247 MPa is around 30% while welding enhances the ultimate stress in HAZ of mile steel with a measured yield stress of 305 MPa by around 13%. Similar findings that the maximum strength reduction in HAZ of high strength steel with a measured yield stress of 780 MPa is around 7% and that of QT steel with a measured yield stress of 1361 MPa is around 45% were reported by Amraei et al. [24] and Jiao et al. [25]. Siltanen et al. [26] found that the maximum reduction of Vickers hardness in HAZ of DQ S960 steel is around 20% while that of QT S960 steel is minor. It is noted that the yield and ultimate stresses linearly increase with increasing hardness [27]. The results indicate that the strength reduction in HAZ could be more significant for higher steel grades and larger for TMCP and DQ high strength steel compared with QT steel.

High heat input in welding of high strength steel could result in severe strength reduction in HAZ while low heat input alleviates the strength reduction or even leads to higher strengths in HAZ of QT steel [23]. The heat input depends on the welding parameters e.g. the current, voltage and welding speed in traditional gas metal arc welding (GMAW), and the applied laser power in laser welding (LW). The heat input of LW could be lower which can result in smaller width of HAZ. Cooling conditions after welding determine the cooling time of HAZ from 800 to 500 °C ($t_{8/5}$) which also strongly affects the material properties of HAZ. Stroetmann et al. [22] found that short cooling time results in significant strength hardening in HAZ of QT S690Q, S960Q and TMCP S500M steel, and the ultimate stresses of HAZ are closer to those of base metals for longer cooling time of 25 seconds. The welding of high strength steel is demanding and vital, but related research remains limited. It is therefore highly desirable to investigate the material properties of HAZ in high strength steel and to provide comprehensive welding guidance in order to avoid excessive material softening in HAZ.

The strength reduction in HAZ of high strength steel could occur in practice. It is therefore necessary to examine the effect of HAZ on the static strength and stiffness of high strength steel CHS X-joints. Numerical simulations were conducted on CHS X-joints in ultra-high steel grades of S900 and S1100 because the strength reduction in HAZ is relatively insignificant for lower steel grades [23-24]. The joint parameters of analysed CHS X-joints are shown in Table 1. The measured geometric parameters and weld sizes of specimens R69 and R75 in tests [17] were adopted herein for FE analysis. The geometric parameters of specimens R69-1 and R75-1 are the same as those of specimens R69 and R75, respectively, expect that the brace and chord walls are thinner to increase the 2γ ratio up to 30.6. The FE models using solid elements and with weld modelling developed by Lan et al. [19] were employed to examine effects of HAZ on CHS X-joints using S900 and S1100 steel.

The width of HAZ in the chord was taken as t_1+w+12 mm as shown in Fig. 2, where t_1 is the brace wall thickness, and w is the weld leg size. The HAZ width was determined in line with the measured micro-hardness profiles in welded ultra-high strength steel tubes with a measured yield stress of 1247 MPa (see Fig. 15 in Javidan et al. [23] for DQ high strength steel). The reduction of yield and ultimate stresses in HAZ near the weld which is in red colour as shown in Fig. 2 was taken as 20% and 30% for S900 and S1100 steel, respectively. The strength reduction of HAZ far from the weld which is in blue colour as shown in Fig. 2 equals to 10% and 15% for steel grades of S900 and S1100, respectively. The magnitudes of strength reduction were determined in accordance with those in DQ high strength steel (see Fig. 2 in Siltanen et al. [26] and Figs. 5-6 in Javidan et al. [23]). The ultimate strain at ultimate stress (ε_u) of HAZ in S900 and S1100 steel near the weld (in red) was taken as 2.1 and 3.5 times of the ultimate strain of base metals, respectively (see Figs. 7 in Javidan et al. [23]). The elastic modulus (E) of HAZ equals to that of base metals. It should be noted that the HAZ was assumed to cover full chord wall thickness in HAZ of specimens R69, R69-1 and R75-1 as the chord walls are relatively thin. The depth of HAZ from the weld in specimen R75 was taken as 12 mm which is the same as the maximum HAZ width from the weld toe due to the thick chord wall with t=22.0 mm. It should be noted that the heat affected zones in the brace were not modelled as the brace cross-section capacity is higher than the joint strength and the failure mode is chord face plastification. The material parameters of base metals of S900 and S1100 steel reported in Ma et al. [28] and those of HAZ in CHS X-joints adopted are shown in Table 2. The value following the letter R denotes the percentage of reduction in yield and ultimate stresses compared with the base metals. The corresponding engineering stress-strain curves adopted which were obtained from the stress-strain curve models proposed by Ma et al. [28] are shown in Figs. 3(b)-(c).

Fig. 4 shows the load-indentation curves of S900 and S1100 steel CHS X-joints without and with HAZ. It is shown that effects of HAZ and steel grades on initial joint stiffness are minor due to almost constant elastic modulus of steel. However, the HAZ reduces the static strength and stiffness of high strength steel CHS X-joints when the brace-chord intersection region becomes plastic and inelastic deformation occurs because of the material strength reduction in HAZ. Table 1 summarises the static strength of analysed CHS X-joints without HAZ (N_{u1}) and with HAZ (N_{u2}). It is shown that the joint strength reduction due to HAZ in S900 steel CHS X-joints varies from 3 to 5% and that for S1100 steel CHS X-joints ranges from 5 to 7%. The reduction of joint strength is relatively insignificant when compared with the large reduction of material strengths in HAZ possibly because the stress in HAZ which becomes plastic could be redistributed to the nearby regions of base metals. Furthermore, the improved yield stress of high strength steel is generally under-utilised in high strength steel CHS X-joints mainly because of the adopted indentation limit, which will be discussed in Section 3.3. This also contributes to the relatively insignificant effect of HAZ on the static strength of CHS X-joints. It is noted that the width and strength reduction of HAZ in DQ high strength steel adopted herein could be smaller if optimised welding parameters are used which could result in negligible strength reduction of CHS X-joints. Additionally, the joint strength reduction of CHS X-joints using QT high strength steel because of HAZ may be smaller than that of CHS X-joints in DQ and TMCP steel because the strength reduction in HAZ of QT steel is less significant [22, 26]. The HAZ is therefore not explicitly modelled in the subsequent parametric study. The strength reduction of CHS X-joints resulted from the HAZ was, however, taken into account by proposing conservative mean strength equations for CHS X-joints using S900 and S1100 steel in Section 4.1.

2.3. Parametric study

There are totally 708 CHS X-joints using S460, S700, S900 and S1100 steel in the parametric study. For each steel grade, 177 specimens were modelled including 81 joint configurations without chord preload and 96 specimens with chord preload. For CHS X-joints without chord preload, the chord diameter (d) is 480 mm. The values of chord wall thickness are 48, 32, 24, 19.2, 16, 13.7, 12, 10.7 and 9.6 mm, and the corresponding ratios (2γ) of chord diameter (d) to wall thickness (t) are 10, 15, 20, 25, 30, 35, 40, 45 and 50. The values of brace diameter (d_1) are 96, 144, 192, 240, 288, 336, 384, 432 and 480 mm with corresponding ratios (β) of brace diameter (d_1) to chord diameter (d) of 0.2, 0.3, 0.4, 0.5, 0.6, 0.7, 0.8, 0.9 and 1.0. Among the specimens without chord preload, 12 joint configurations with 2γ ratios of 10, 25 and 40, and β ratios of 0.3, 0.5, 0.7 and 0.9 were selected to examine effects of chord preload ratio (n) which equals to the ratio of chord preload (N_p) to chord cross-section yield load (Af_y). Eight values of n ratio of -0.8, -0.6, -0.4, -0.2, 0.2, 0.4, 0.6 and 0.8 were analysed. Negative and positive values of n ratio denote chord compression and tension, respectively. The angle between brace and chord members (θ) and the ratio (τ) of brace wall thickness (t_1) to chord wall thickness (t) were set to be 90° and 1.0, respectively. This is because these two parameters have minor effect on the strength ratio of mean strengths predicted by EN 1993-1-8 [1] and the CIDECT design guide [3] to numerical or test strengths of high strength steel CHS X-joints [19]. The length of chord members (l) was taken as $6d$ and that of brace members (l_1) was set to be $3d_1$, in accordance with those adopted by Lan et al. [19]. The investigated parameter ranges in the parametric study are $0.2 \leq \beta \leq 1.0$, $10 \leq 2\gamma \leq 50$ and $-0.8 \leq n \leq 0.8$.

It is noted that the CHS X-joint specimens tested by Puthli et al. [17] were made of hot-finished steel CHS tubes. The values of yield stress (f_y) and ultimate stress (f_u) of S460 steel in the parametric study were taken as the average values of f_y and f_u of chord members of specimens R45, R60, R61, R62, R63 and R73 using S460 steel under axial compression [17]. However, elastic modulus (E), ultimate strain at ultimate stress (ε_u) and stress-strain curves of the specimens [17] were not reported. Thus, the value of elastic modulus (E) was taken as 210 GPa, in accordance with EN 1993-1-1 [29]. The ultimate strain at ultimate stress (ε_u) of S460 steel was determined by the predictive equation proposed by Yun and Gardner [30]. The bi-linear plus nonlinear hardening material model [30] for hot-finished steel was adopted for S460 steel. The material parameters and stress-strain curve models of cold-formed CHS using S700, S900 and S1100 steel reported by Ma et al. [28] were used in the numerical analysis. Table 2 summarizes the material parameters used for high strength steel. Fig. 3 shows the engineering stress-strain curves adopted, which are based on the material models proposed by Yun and Gardner [30] and Ma et al. [28].

The validated FE models using the shell element S4R and without weld modelling [19] were adopted for the parametric study. The mesh size was determined by a mesh convergence study. It is found that a mesh size of 16 mm for the specimens in the parametric study is suitable. For CHS X-joints without chord preload, all degrees of freedom at the end of two braces were restricted, except for axial displacement at the two brace ends, and the two chord ends were free to translate and rotate. The axial compressive loading at the end of brace members was applied by displacement. For CHS X-joints with chord preload, all degrees of freedom at the brace and chord ends were constrained, except for the axial displacement. The chord preload was firstly applied to the chord and then the brace ends were loaded by displacement. Results of parametric analysis in this study and experimental tests [17, 18] were used to assess current design provisions and to propose design rules for high strength steel CHS X-joints.

3. Comparison and evaluation of design rules

3.1. Current design rules

Design provisions for normal strength steel tubular joints specified in EN 1993-1-8 [1] and ANSI/AISC 360-10 [7] are generally in accordance with design rules proposed by Wardenier [31] and the 2nd edition of the IIW recommendations [32]. There is no deformation limit considered and the design rules are primarily based on test results. The CIDECT design guide [3] and ISO 14346 [4] are generally in line with the 3rd edition of the IIW recommendations [5], and the indentation limit of 3%*d* is adopted. The design equations for tubular joints [3-5] are mainly based on FE database because test data inevitably include a certain amount of scatter while FE results could avoid such scatter [33]. API RP 2A WSD [6] employs the Yura displacement limit which is $60d_1f_y/E$ for axially loaded tubular joints, and the design equations are developed from regression analysis using the MSL screened test database, the unscreened test database compiled by Kumamoto University and the API/EWI validated FE database [34]. The design codes and guides [1, 3-7, 32] are applicable for hot-finished and cold-formed steel tubular joints, and the general format of the strength equation for axially loaded CHS X-joints which fail by chord plastification is as follows:

$$N_{1,\mathrm{u}} = Q_\mathrm{u} Q_\mathrm{f} \frac{f_\mathrm{y} t^2}{\sin\theta} \tag{1}$$

where the reference strength equation (Q_u) is expressed as a function of γ and β, and the chord stress equation (Q_f) accounts for the effect of chord longitudinal stresses on the joint strength.

It is noted that the reference strength equations (Q_u) adopted for CHS X-joints using normal strength steel [1, 3-5, 7, 32] are based on the ring model as shown in Fig. 5 [35, 36]. The ring model assumes that most of the loads applied in the braces are transferred at the saddle (see Fig. 5(a)). It also postulates that the brace loading is resisted by the six plastic hinges at the assumed positions, and the effects of axial and shear stresses on the plastic moment resistance of the plastic hinge could be neglected. It is also noted that effects of strain-hardening and membrane action in chord members are not taken into account in the ring model. The chord plastification failure of CHS X-joints is mainly caused by the load component ($N_1\sin\theta$), which is perpendicular to the chord, of the brace loading (N_1). In the ring model, the load component ($N_1\sin\theta$) is divided into two loads ($0.5N_1\sin\theta$) at point A. The distance between the two plastic hinges at point A as shown in Fig. 5(a) is assumed to be Bd_1 (B<1.0). The failure mode of chord plastification could be represented by a fourth model (see Fig. 5(b)) due to symmetry, in which the load ($0.5N_1\sin\theta$) at each plastic hinge is transferred by an effective length (B_e) along the chord longitudinal direction as shown in Fig. 5(c). The plastic moment capacity (M_p) of each plastic hinge equals to $B_et^2f_y/4$. The reference strength equation (Q_u) for CHS X-joints can be obtained from the moment equilibrium equation in Fig. 5(b) as follows [35]:

$$Q_\mathrm{u} = \frac{2B_\mathrm{e}/d}{1-B\beta} \tag{2}$$

The effective length (B_e) which is dependent on β and γ ratios can be determined by regression analysis using test or numerical database. Thus, Eq. (2) can be expressed as follows [30]:

$$Q_\mathrm{u,EC} = \frac{A}{1-B\beta}\gamma^{C\beta-D\beta^2} \tag{3}$$

$$Q_\mathrm{u,CIDECT} = \frac{A+E\beta}{1-B\beta}\gamma^{C} \tag{4}$$

where A, B, C, D and E are regression coefficients. It is noted that EN 1993-1-8 [1], ANSI/AISC 360-10 [7] and the IIW recommendations [32] adopt Eq. (3) for the regression analysis using test data. The CIDECT design guide [3], ISO 14346 [4] and the IIW recommendations [5] employ Eq. (4) which simplifies the quadratic function of β in the exponent of Eq. (3) for the regression analysis using numerical results of

S355 CHS X-joints. It should be noted that the difference between the peak load and the load at the indentation limit of 3%*d* is generally small for normal strength steel CHS X-joints under zero or compressive chord preload [36]. This therefore indicates that in general the indentation limit is not a governing factor limiting the joint strength and the plastic hinges could effectively form at the assumed positions (see Fig. 5(a)) when the joint strength is controlled by the indentation limit.

The chord stress equations (Q_f) in design codes and guides [1, 3-7, 32] for normal strength steel CHS X-joints are obtained from regression analysis which generally adopts lower bounds of test or numerical data [31, 34, 36]. It is noted that chord stress equations adopted by EN 1993-1-8 [1], API RP 2A WSD [6], ANSI/AISC 360-10 [7] and the IIW recommendations [32] account for the detrimental effect of compressive chord axial stresses on joint strength (i.e. Q_f<1.0). However, no reduction of joint strength (i.e. Q_f=1.0) is prescribed for tensile chord axial stresses. van der Vegte et al. [36] numerically examined the effect of chord preload on the static strength of CHS X-joints in S355 steel and found that large tensile chord axial stresses could also result in significant reduction of the joint strength. Based on the numerical results, a new chord stress equation which can consider the effect of compressive and tensile chord axial stresses was proposed as follows [36]:

$$Q_f = (1.0 - |n|^F)^{G+H\beta+J\gamma} \quad (5)$$

where *F*, *G*, *H* and *J* are regression coefficients. The CIDECT design guide [3], ISO 14346 [4] and the IIW recommendations [5] adopt the format of Eq. (5) to account for the effect of chord axial stresses.

It should be noted that the regression analysis of test or numerical data for the reference strength equation (Q_u) and the chord stress equation (Q_f) leads to the mean strength equations for CHS X-joints using normal strength steel. The mean strength equations can be converted to characteristic strength equations by considering fabrication tolerances, mean values and scatter of test or numerical data and a correction of steel yield stress [33]. The design strength equations [1, 3-5, 32] can be derived from the characteristic strength equations divided by a safety factor which is 1.1 for CHS X-joints which fail by chord face plastification. The commentary K3 of ANSI/AISC 360-10 [7] indicates that the available axial strength equations specified for CHS X-joints are characteristic strength equations. Procedures of converting mean to design strength equations are detailed in Wardenier [31] and van der Vegte et al. [33].

3.2. Comparison with numerical and test results

The failure mode of high strength steel CHS X-joints analysed in Section 2.3 and those tested by Puthli et al. [17] and Lee et al. [18] (see Table 3) is chord plastification. The indentation limit of 3%*d* was adopted in this study and experimental tests [17, 18]. It is also noted that the design rules for normal strength steel CHS X-joints subjected to brace axial compression specified in the CIDECT design guide [3] are the same as those in ISO 14346 [4] and the IIW recommendations [5]. The CIDECT design strength ($N_{CIDECT,Rd}$) can be obtained from:

$$N_{CIDECT,Rd} = 2.6\left(\frac{1+\beta}{1-0.7\beta}\right)\gamma^{0.15} Q_{f,CIDECT} \frac{f_y t^2}{\sin\theta} \quad (6)$$

$$Q_{f,CIDECT} = (1-|n|)^C \quad (7)$$

$$C = \begin{cases} 0.45 - 0.25\beta & \text{for n<0} \\ 0.20 & \text{for } n \geq 0 \end{cases} \tag{8}$$

where β is the ratio of brace diameter (d_1) to chord diameter (d), γ is the ratio of chord diameter (d) to twice chord wall thickness (t), θ is the angle between the brace and chord members, f_y is the yield stress of the chord, $Q_{f,CIDECT}$ is the chord stress equation, and n is the chord preload ratio. Negative and positive values of n denote compressive and tensile chord axial stresses, respectively. To allow for objective and consistent comparison, the CIDECT mean strength equation which is based on the numerical analysis conducted by van der Vegte [33, 36] was adopted as follows:

$$N_{\text{CIDECT,Mean}} = 1.215 \times 2.6(\frac{1+\beta}{1-0.7\beta})\gamma^{0.15} Q_{\text{f,CIDECT}} \frac{f_y t^2}{\sin\theta} \tag{9}$$

It is noted that an implicit safety factor of 1.215 was incorporated in the design strength equation (Eq. (6)) compared with the mean strength equation (Eq. (9)).

Fig. 6 shows the comparison of CIDECT mean strengths ($N_{CIDECT,Mean}$) calculated from Eq. (9) with numerical strengths obtained in Section 2.3 (N_{FE}) and test strengths summarized in Table 3 (N_{Test}) for CHS X-joints without chord preload. Figs. 7-10 show the comparison of the joint strength reduction predicted by Eq. (7) ($Q_{f,CIDECT}$) with that obtained from finite element simulations in this study ($Q_{f,FE}$) for CHS X-joints subjected to chord preload. It should be noted that the reduction of joint strength (Q_f) is defined as the ratio of the static strength of tubular joints to that of the same joints without chord preload.

3.3. Assessment of the CIDECT design rules

3.3.1. CHS X-joints without chord preload

This subsection evaluates the applicability of the CIDECT mean strength equation (Eq. (9)) for high strength steel CHS X-joints without chord preload, in which $Q_{f,CIDECT}$=1.0. Fig. 6 shows that $N_{CIDECT,Mean}/N_{FE}$ and $N_{CIDECT,Mean}/N_{Test}$ ratios generally increase with increasing yield stress (f_y). Table 4 summarizes mean values and coefficients of variation (COV) of $N_{CIDECT,Mean}/N_{FE}$ ratio for CHS X-joints without chord preload. The mean values of $N_{CIDECT,Mean}/N_{FE}$ ratio for steel grades S460, S700, S900 and S1100 are 1.01, 1.17, 1.35 and 1.40 with corresponding COV of 0.073, 0.085, 0.128 and 0.156. The mean value of $N_{CIDECT,Mean}/N_{Test}$ ratio (see Table 3) for steel grades ranging from S460 to S770 is 1.15 with corresponding COV of 0.080. It is shown that the CIDECT mean strength prediction is slightly unconservative and consistent for S460 CHS X-joints without chord preload. However, the CIDECT mean strength equation (Eq. (9)) which is dependent on f_y and ratios of β, γ and n generally produces increasingly unconservative and scattered strength prediction for steel grades greater than S460.

Fig. 11 examines effects of β and 2γ ratios on $N_{CIDECT,Mean}/N_{FE}$ ratio of CHS X-joints without chord preload. It should be noted that the validity ranges of β and 2γ ratios for the CIDECT design and mean strength equations (Eqs. (6-9)) are $0.2 \leq \beta \leq 1.0$ and $2\gamma \leq 40$. Fig. 11(a) shows that in general $N_{CIDECT,Mean}/N_{FE}$ ratio of CHS X-joints using S460 steel slightly decreases and then increases with increasing β ratio up to 0.9 and decreases for β=1.0. The $N_{CIDECT,Mean}/N_{FE}$ ratio increases with increasing 2γ ratio for β=0.2 and with decreasing 2γ ratio for β=1.0. The effect of 2γ ratio on $N_{CIDECT,Mean}/N_{FE}$ ratio is relatively insignificant for $0.3 \leq \beta \leq 0.9$. It is shown that the CIDECT mean strength prediction is, in general, reasonably accurate and slightly unconservative for S460 CHS X-joints with β and 2γ ratios which are within the CIDECT validity ranges. Fig. 11(b) shows that $N_{\mathrm{CIDECT,Mean}}/N_{\mathrm{FE}}$ ratio of CHS X-joints using S700 steel generally decreases and then slightly increases with increasing β ratio up to 0.9 and decreases for β=1.0. The $N_{\mathrm{CIDECT,Mean}}/N_{\mathrm{FE}}$ ratio increases with increasing 2γ ratio for $0.2\leq\beta\leq0.5$ and with decreasing 2γ ratio for β=1.0. The effect of 2γ ratio on $N_{\mathrm{CIDECT,Mean}}/N_{\mathrm{FE}}$ ratio is relatively insignificant for $0.6\leq\beta\leq0.9$. It is noted that the CIDECT mean strength prediction is relatively accurate for β=1.0, except that the prediction for the CHS X-joint with 2γ=10 is relatively unconservative. In general, the CIDECT mean strength prediction is unconservative for S700 CHS X-joints. Figs. 11(c)-(d) show that $N_{\mathrm{CIDECT,Mean}}/N_{\mathrm{FE}}$ ratio of CHS X-joints using S900 and S1100 steel generally decreases with increasing β ratio. The $N_{\mathrm{CIDECT,Mean}}/N_{\mathrm{FE}}$ ratio generally increases with increasing 2γ ratio for $0.2\leq\beta\leq0.9$ and with decreasing 2γ ratio for β=1.0. It is also noted that the CIDECT mean strength prediction is relatively accurate for β=1.0, except that the prediction for the CHS X-joint with 2γ=10 is relatively unconservative. It is shown that the CIDECT mean strength prediction is generally unconservative for CHS X-joints using S900 and S1100 steel.

The load applied in the braces is primarily resisted by the bending action of the chord of the CHS X-joints with small to medium β ratio, and thus the joint deformation is mainly concentrated in the vicinity of the brace perimeter. The corresponding joint strength is generally determined by the load at the indentation limit of 3%d instead of the peak load (i.e. deformation-controlled). The deformation of CHS X-joints using the same steel depends on the joint axial stiffness, which increases with increasing β ratio and with decreasing 2γ ratio [37]. Consequently, the CHS X-joints with larger β ratio and lower 2γ ratio could be subjected to larger brace loadings and thus higher stresses before the violation of the indentation limit because of larger joint stiffness, and therefore the increased yield stress of high strength steel could be utilised more effectively. The ring model on which the CIDECT mean strength equation is based assumes that the stresses in the region of the plastic hinges could reach the yield stress (f_y) as discussed in Section 3.1. The CIDECT mean strength prediction is therefore generally more accurate and consistent for the CHS X-joints with larger β ratio and lower 2γ ratio. In contrast, the axial compression in the braces of the CHS X-joints with β ratio approaching or equal to 1.0 is mainly transferred through the compressive axial stress in the chord wall between the two braces. The corresponding joint strength is generally determined by the peak load which is controlled by the cross-section yielding of the chord wall between the two braces. Thus, the increased yield stress of high strength steel could be used more effectively, and the CIDECT mean strength prediction is generally accurate for the CHS X-joints with β=1.0.

Fig. 12 further compares representative load-indentation curves of CHS X-joints without chord preload to investigate the effect of steel grade on $N_{\mathrm{CIDECT,Mean}}/N_{\mathrm{FE}}$ ratio. Fig. 13 shows typical yielding patterns of CHS X-joints with β=0.5 and 2γ=25 at the determined joint strengths. The highly strained areas in the brace-chord intersection regions (in red and green colours) and the middle of the chord (in light blue) became plastic. Figs. 12(a)-(b) show that large inelastic deformation occurs in S460 CHS X-joints with low and medium β ratios (i.e. 0.2 and 0.5) and 2γ=25 when the indentation exceeds the indentation limit of 3%d. Fig. 13(a) demonstrates that the onset of plasticity has taken place, and the plastic hinges assumed in the ring model (see Fig. 5(a)) is in the process of developing at the indentation limit. This indicates that the CIDECT mean strength equation which is based on the ring model is generally applicable for S460 CHS X-joints. Thus, the CIDECT strength prediction is, in general, reasonably accurate and slightly unconservative as shown in Fig. 11(a). The slightly unconservative prediction is possibly due to the plastic hinges which were not fully developed at the indentation limit. However, the CHS X-joints using higher steel grades S700, S900 and S1100 could be subjected to increasingly higher elastic stresses before stresses within the joints reach the corresponding yield stresses. It is noted that the initial stiffness of the same joints using different steel grades is almost the same as shown in Fig. 12 due to nearly constant elastic modulus of normal and high strength steel. Therefore, only small inelastic deformation could take place for the CHS X-joints using steel grade S700, and the deformation of the CHS X-joints using steel grades S900 and S1100 is largely elastic as shown in Figs. 12(a)-(b). The corresponding yielding patterns are shown in Figs. 13(b)-(d). It is shown that the plastic hinges in the middle of the chord could not fully develop for steel grades S700, S900 and S1100, and the effective length (B_e) along the chord longitudinal direction of the plastic hinge (see Fig. 5(c)) is increasingly short with increasing steel grade. Thus, the CIDECT mean strength equation produces increasing unconservative and scattered strength prediction for the CHS X-joints using steel grades S700, S900 and S1100 (see Figs. 11(b)-(d)). Fig. 12(c) shows that large inelastic deformation occurs at the indentation limit for CHS X-joints using steel grades S460, S700, S900 and S1100 when β=1.0 and 2γ=25. It is noted that the corresponding joint strengths were determined by the peak loads and thus the indentation limit is not a governing factor limiting the joint strengths. This indicates that the plastic hinges could fully develop and thus the CIDECT mean strength equation is relatively accurate (see Fig. 11). Fig. 12(d) shows that large inelastic deformation takes place at the indentation limit for CHS X-joints using steel grades S460, S700, S900 and S1100 when β=1.0 and 2γ=10 while the joint strength is deformation-controlled. This is similar to the cases of S460 CHS X-joints with low and medium β ratios and 2γ=25. The corresponding CIDECT mean strength prediction is, therefore, relatively accurate and somewhat unconservative as shown in Fig. 11.

3.3.2. CHS X-joints with chord preload

The suitability of CIDECT chord stress equation (Eq. (7)) for high strength steel CHS X-joints subjected to chord preload was assessed. Figs. 7-10 show that the CIDECT prediction of joint strength reduction ($Q_{f,CIDECT}$) is increasingly conservative with increasing chord preload ratio (n). Table 5 summarizes mean values and COV of the ratio ($Q_{f,CIDECT}/Q_{f,FE}$) of joint strength reduction predicted by the CIDECT chord stress equation (Eq. (7)) ($Q_{f,CIDECT}$) to that obtained in numerical analysis ($Q_{f,FE}$) for CHS X-joints subjected to chord preload. The mean values of $Q_{f,CIDECT}/Q_{f,FE}$ ratio for steel grades S460, S700, S900 and S1100 are 0.93, 0.91, 0.89 and 0.88 with corresponding COV of 0.059, 0.056, 0.065 and 0.076. It is shown that the CIDECT chord stress equation is increasingly conservative with increasing steel grade. This is because the increased yield stress of high strength steel generally could not be fully utilised for CHS X-joints without chord preload, and thus the effect of chord preload on the joint strength becomes increasingly insignificant with increasing steel grade. It should be noted that the CIDECT chord stress equation is obtained from regression analysis using FE database of CHS X-joints using S355 steel, and the corresponding joint strength is generally determined by the load at the indentation limit for tensile chord preload and the peak load for zero or compressive chord preload [36]. Figs. 7-10 also show that the effect of chord preload ratio (n) is dependent on β and 2γ ratios. For the CHS X-joints with small to medium β ratio (e.g. β=0.3, 0.5 and 0.7), when the chord wall bends, the membrane action develops resulting in tensile chord axial stresses which can resist the compressive brace loading and thus enhance the joint strength. Small enhancement of the joint strength (i.e. $Q_{f,FE}$>1.0) is, therefore, observed in Figs. 7-10 for small tensile chord preload while the compressive chord preload generally reduces the joint strength (i.e. $Q_{f,FE}$<1.0). For the CHS X-joints with large β ratio (e.g. β=0.9), the brace loading is mainly transferred in the chord wall between the two braces. The compressive chord preload slightly increases the joint strength for small compressive chord preload while the tensile chord preload lowers the joint strength. This is because a combination of compressive stresses in perpendicular directions results in a higher yield stress than a combination of compressive and tensile stresses according to the von Mises yield criterion. The value of $Q_{\mathrm{f,FE}}$ generally decreases with increasing 2γ ratio when n≤0 and with decreasing of 2γ ratio when n>0. The effect of 2γ ratio is relatively insignificant for relatively small chord preload ratio.

4. Proposed design rules for high strength steel CHS X-joints

4.1. Proposed mean strength equation

The mean strength equation for high strength steel CHS X-joints was proposed by modifying the CIDECT mean strength equation (Eq. (9)). The analysis described in Section 3.3 shows that in general the increased yield stress of high strength steel could not be fully utilised for CHS X-joints with large 2γ ratio, and thus the CIDECT mean strength prediction is generally unconservative and scattered. It is therefore proposed to limit the range of 2γ ratio to avoid applying small reduction factors of joint strength to the CIDECT mean strength equation for high strength steel CHS X-joints which largely eliminate the benefits of using high strength steel. It is suggested that the 2γ ratio should not be greater than 40 for steel grades ranging from S460 to S700, which is consistent with the validity range of 2γ ratio for CHS X-joints using steel grades up to S460 specified in the CIDECT design guide [3]. For steel grades greater than S700 and up to S1100, the range of 2γ ratio is recommended to be within 30. The proposed recommendation is also in line with the design philosophy of the CIDECT design guide [3] which suggests choosing relatively stocky cross-sections for chord members to avoid local buckling of the chord in compression and to reduce the painting for fire and corrosion protection. The CIDECT design guide [3] stipulates that the chord of CHS X-joints under compression should be Class 1 or 2. The proposed limits of 2γ ratio for CHS X-joints using steel grades ranging from S460 to S1100 are also within the plastic slenderness limits of CHS cross-sections proposed by Ma et al. [38] which are 54, 44, 37 and 35 for steel grades S460, S700, S900 and S1100, respectively. The effect of β ratio on $N_{\mathrm{CIDECT,Mean}}/N_{\mathrm{FE}}$ ratio becomes less significant when 2γ ratio is within the suggested limits (see Fig. 11). Therefore, the suggested range of β ratio for CHS X-joints using steel grades ranging from S460 to S1100 is $0.2\leq\beta\leq1.0$, which is the same as the current CIDECT validity range of β ratio.

In general, the CIDECT mean strength prediction is unconservative for CHS X-joints without chord preload and the joint strength reduction predicted by Eq. (7) ($Q_{\mathrm{f,CIDECT}}$) is conservative for CHS X-joints under chord preload when β and 2γ ratios are within the proposed limits (see Figs. 7-11). Regression analysis of numerical results obtained in this study was conducted to propose mean strength equation for CHS X-joints using steel grades ranging from S460 to S1100 as follows:

$$N_{\mathrm{Proposed,Mean}} = 3.16\left(\frac{1+\beta}{1-0.7\beta}\right)\gamma^{0.15}Q_{\mathrm{y}}Q_{\mathrm{f,Proposed}}\frac{f_{\mathrm{y}}t^{2}}{\sin\theta} \tag{10}$$

$$Q_{\mathrm{y}} = -62 f_{\mathrm{y}} / E + 1.1 \tag{11}$$

$$Q_{\mathrm{f,Proposed}} = (1-|n|)^{\alpha C} \tag{12}$$

$$\alpha = -84 f_{\mathrm{y}} / E + 1.0 \tag{13}$$

The proposed reduction factor of joint strength (Q_{y}) which decreases with increasing yield stress (f_{y}) and with decreasing elastic modulus (E) accounts for the under-utilisation of the increased yield stress of high strength steel. The proposed reduction factors for steel grades S460, S700, S900 and S1100 investigated in this study are 0.95, 0.88, 0.79 and 0.75, respectively. It should be noted that the proposed reduction factor of joint strength (Q_y) may be conservative for the mean strength prediction of CHS X-joints with large β and 2γ ratios (see Fig. (11)). The deformation capacity of CHS X-joints with large β and 2γ ratios is, however, relatively low (see Fig. 12 (c)), and thus application of the conservative reduction factors of joint strength could limit the joint deformation occurring in practice. It should be noted that Kurobane et al. conducted regression analysis of test results and proposed a mean strength equation for CHS X-joints in which the function of yield ratio (f_y/f_u) of yield stress (f_y) to ultimate stress (f_u) is as follows [31]:

$$f = \left(\frac{f_y}{f_u}\right)^{-0.173} \tag{14}$$

The yield ratio of high strength steel analysed in the numerical study and experimental tests [17, 18] varies from 0.74 to 0.98 with corresponding f value ranging from 1.05 to 1.00. This indicates that the effect of yield ratio on the static strength of CHS X-joints is insignificant. Thus, the effect of yield ratio was not explicitly considered in the proposed mean strength equation (Eq. (10)).

The joint strengths calculated from the proposed mean strength equation ($N_{Proposed,Mean}$) were compared with the test strengths (N_{Test}) and numerical strengths (N_{FE}) for CHS X-joints without chord preload. It should be noted that values of elastic modulus of the high strength steel [17, 18] summarized in Table 3 were not reported, and thus the value was taken as 210 GPa in accordance with EN 1993-1-1 [29]. Tables 3-4 show results of statistical analysis for $N_{Proposed,Mean}/N_{Test}$ and $N_{Proposed,Mean}/N_{FE}$ ratios. The mean value of $N_{Proposed,Mean}/N_{Test}$ ratio is 1.01 with corresponding COV of 0.067. The mean values of $N_{Proposed,Mean}/N_{FE}$ ratio for steel grades S460, S700, S900 and S1100 are 0.97, 1.02, 1.01 and 0.98 with corresponding COV of 0.065, 0.074, 0.085 and 0.107. It is shown that the proposed mean strength equation (Eq. (10)) can produce accurate and consistent strength prediction for high strength steel CHS X-joints. The curves of the proposed chord stress equation (Eq. (12)) are shown in Figs. 7-10. It is shown that the joint strength reduction predicted by Eq. (12) ($Q_{f,Proposed}$) is more accurate than that obtained from the CIDECT chord stress equation (Eq. (7)) ($Q_{f,CIDECT}$) when compared with the FE results ($Q_{f,FE}$). Table 5 shows results of statistical analysis for $Q_{f,Proposed}/Q_{f,FE}$ ratio. The mean values of $Q_{f,Proposed}/Q_{f,FE}$ ratio for steel grades S460, S700, S900 and S1100 are 0.96, 0.99, 0.99 and 0.98 with corresponding COV of 0.052, 0.059, 0.043 and 0.036. It is shown that the proposed chord stress equation (Eq. (12)) is reasonably accurate and slightly conservative. Table 6 summarizes results of statistical analysis for CHS X-joints without and with chord preload investigated in Section 2.2. It is shown that in general the CIDECT mean strength prediction is unconservative and scattered with mean value and COV of 1.17 and 0.176, respectively, and the strength prediction produced by the proposed mean strength equation (Eq. (10)) is relatively accurate and consistent with mean value and COV of 0.98 and 0.126, respectively. It should be noted that the proposed mean strength equation is conservative for CHS X-joints using steel grades of S900 and S1100 to consider the joint strength reduction resulted from the HAZ as discussed in Section 2.2. Data of CHS X-joints with n=-0.8 were not included in the statistical analysis for $N_{CIDECT,Mean}/N_{FE}$ and $N_{Proposed,Mean}/N_{FE}$ ratios in Table 6 as such data points may exhibit large errors in percentage terms, in accordance with van der Vegte et al. [36]. CHS X-joints with 2γ ratio greater than the suggested limits were also excluded in the statistical analysis for $N_{Proposed,Mean}/N_{FE}$ and $Q_{f,Proposed}/Q_{f,FE}$ ratios in Tables 4-6.

4.2. Determination of design strengths

Procedures of converting mean to design strengths employed by the IIW recommendations [5, 32] are described in Wardenier [31] and van der Vegte et al. [33]. The same procedure was adopted herein. The characteristic strength ($N_{u,k}$) converted from mean strength ($N_{u,m}$) is determined by considering fabrication tolerances, mean values and scatter of data, and a correction factor of yield stress. The characteristic strength ($N_{u,k}$) for a large number of data with 5% probability of lower strengths is as follows [31, 33]:

$$N_{u,k} = N_{u,m}(1-1.64V_{N_u})\frac{f_{y,m}}{f_{y,k}} \tag{15}$$

$$V_{N_u} = \frac{\left[\mathrm{VAR}(N_u)\right]^{0.5}}{N_u} \tag{16}$$

$$\mathrm{VAR}(N_u) = N_u^2\left[(\frac{s_{f_y}}{f_y})^2 + (1.85\frac{s_t}{t})^2 + (\frac{s_\delta}{\delta})^2\right] \tag{17}$$

where the ratio of mean to design yield stresses ($f_{y,m}/f_{y,k}$) was taken as 1/0.85, and the values of standard deviation of yield stress (s_{fy}/f_y) and chord wall thickness (s_t/t) were taken as 0.075 and 0.05, respectively, in accordance with van der Vegte et al. [33]. The highest mean and COV values of 216 CHS X-joints without chord preload in Table 4 and 320 CHS X-joints under chord preload in Table 5 were adopted (i.e. mean=0.99 and s_δ/δ=0.084). The characteristic strength ($N_{u,k}$) can be obtained by substituting Eqs. (16-17) into Eq. (15) followed by a correction of the mean value as follows [33]:

$$N_{u,k} = N_{u,m}\times(1-1.64\times0.15)\times\frac{1}{0.85}\times\frac{1}{0.99} = 0.90N_{u,m} \tag{18}$$

It is noted that CHS X-joints investigated in this study failed by ductile failure mode of chord plastification, and thus a safety factor (γ_m) could be taken as 1.1 [31, 33]. The design strength can be obtained from:

$$N_{u,Rd} = \frac{N_{u,k}}{\gamma_m} = 0.82N_{u,m} \tag{19}$$

Thus, the proposed design strength equation for CHS X-joints using steel grades ranging from S460 to S1100 which fail by chord plastification is as follows:

$$N_{Proposed,Rd} = 2.6(\frac{1+\beta}{1-0.7\beta})\gamma^{0.15}Q_y Q_{f,Proposed}\frac{f_y t^2}{\sin\theta} \tag{20}$$

The validity range of 2γ ratio is 2γ≤40 for steel grades ranging from S460 to S700 and 2γ≤30 for steel grades greater than S700 and up to S1100, and that of β ratio is 0.2≤β≤1.0 for steel grades ranging from S460 to S1100. It is noted that the CIDECT design strength equation (Eq. (6)) modified by the proposed reduction factor of joint strength (Eq. (11)) and chord stress function (Eq. (12)) is the same as the proposed design strength equation (Eq. (20)).

It should be noted that the proposed mean and design strength equations for high strength steel CHS X-joints which failed by chord plastification implicitly incorporated the indentation limit i.e. 3% of chord diameter (d). Adopting the indentation limit originally proposed by Lu et al. [21] for normal strength steel tubular joints is the longstanding CIDECT practice. Such indentation limit serves to control joint deformations at ultimate and serviceability limit states because of the high flexibility of some CHS joints [3]. It is noted that in general the indentation limit is not a governing factor limiting the joint strength for normal strength steel CHS X-joints under zero or compressive chord load [36]. In general, the static strength of the majority of high strength steel CHS X-joints analysed in this study was, however, determined by the load at the indentation limit, and thus the increased yield stress of high strength steel could not be effectively utilised. It is significant to investigate whether the indentation limit could be further relaxed for high strength steel tubular joints to allow for more effective use of high strength steel. This therefore necessitates studies to examine the joint deformation occurring at the ultimate and serviceability limit states of high strength steel tubular structures in practice. It is also noted that the increased yield ratio and low ductility of high strength steel may affect the redistribution of stresses and thus secondary bending moments in tubular structures which are usually neglected in structural analysis. Therefore, in addition to the investigation on isolated tubular joints herein, comparative research on the structural behaviour of high strength steel tubular joints in tubular structures is needed. Indeed, there are commercially available high strength steel CHS tubes with 2γ ratio which falls outside the suggested limits. Various reinforcing methods could be adopted to enhance the joint stiffness of CHS joints with large 2γ ratios and thus to utilise high strength steel more effectively such as internal ring stiffeners [39, 40], external stiffeners [41], collar plates [42], doubler plates [43] and grouting concrete [44, 45]. Further research on high strength steel reinforced tubular joints is needed.

5. Conclusions

The structural behaviour and static strength of CHS X-joints using steel grades ranging from S460 to S1100 under axial compression in the braces were studied. Numerical simulations covering a wide range of geometric parameters and chord preload ratios were carried out. The investigated failure mode of the CHS X-joints is chord plastification. Effects of heat affected zones (HAZ) on the CHS X-joints were examined. Suitability of the mean strength equation adopted by the CIDECT design guide for the CHS X-joints was evaluated against results obtained from the numerical simulations in this study and experimental tests in the literature. Influences of the steel grade, brace to chord diameter ratio (β), chord diameter to wall thickness ratio (2γ) and chord preload ratio (n) on the applicability of the CIDECT mean strength equation for the CHS X-joints were assessed. Design rules were proposed for the CHS X-joints. The conclusions are summarized as follows:

(1) The effect of HAZ on the initial stiffness of the CHS X-joints is minor and the HAZ could lower the static strength of the CHS X-joints. However, the joint strength reduction resulted from the HAZ is relatively insignificant.

(2) The CIDECT mean strength prediction, in general, is slightly unconservative for steel grade S460 and becomes increasingly unconservative with increasing steel grade, and is increasingly unconservative with decreasing β ratio and with increasing 2γ ratio. The CIDECT prediction of joint strength reduction resulted from the chord preload is increasingly conservative with increasing n ratio and steel grade.

(3) The improved yield stress of high strength steel generally could not be fully utilised which results in the unconservative CIDECT mean strength prediction for the CHS X-joints. The under-utilisation of high strength steel is mainly due to the adopted indentation limit i.e. 3% of chord diameter.

(4) The recommended ranges of 2γ ratio are $2\gamma \leq 40$ for steel grades ranging from S460 to S700 and $2\gamma \leq 30$ for steel grades greater than S700 and up to S1100 to allow for more effective use of high strength steel. The suggested range of β ratio is $0.2 \leq \beta \leq 1.0$ for steel grades ranging from S460 to S1100.

(5) A mean strength equation was proposed for the CHS X-joints with 2γ and β ratios which are within the suggested ranges. The proposed mean strength equation can produce reasonably accurate and

consistent strength prediction. The proposed mean strength equation was converted to a design strength equation for the design of high strength steel CHS X-joints.

Acknowledgements

The authors appreciate the support from the Chinese National Engineering Research Centre for Steel Construction (Hong Kong Branch) at The Hong Kong Polytechnic University. The financial support from The Hong Kong Polytechnic University (PolyU: 1-ZE50/G-YBUU) is also gratefully acknowledged. The first author is also grateful for the support given by the Research Grants Council of Hong Kong for the Hong Kong PhD Fellowship Scheme.

References

[1] Eurocode 3 (EC3), Design of Steel Structures-Part 1–8: Design of Joints. European Committee for Standardization, EN 1993-1-8, CEN, Brussels, 2005.

[2] J.A. Packer, J. Wardenier, X.L. Zhao, G.J. van der Vegte, Y. Kurobane, Design Guide for Rectangular Hollow Section (RHS) Joints Under Predominantly Static Loading, CIDECT, Verlag TUV Rheinland, Cologne, Germany, 2009.

[3] J. Wardenier, Y. Kurobane, J.A. Packer, G.J. van der Vegte, X.L. Zhao, Design Guide for Circular Hollow Section (CHS) Joints under Predominantly Static Loading, CIDECT, Verlag TUV Rheinland, Cologne, Germany, 2008.

[4] ISO. Static design procedure for welded hollow-section joints-Recommendations. ISO/FDIS 14346: 2012(E), Geneva.

[5] International Institute of Welding (IIW) Subcommission XV-E, XV-1281-08: Static Design Procedure for Welded Hollow Section Joints-Recommendations, 3rd Ed., 2008.

[6] American Petroleum Institute (API), Recommended practice for planning, designing and constructing fixed offshore platforms-working stress design, API Recommended Practice 2A WSD (RP 2A WSD), 22nd Ed., 2014 (Washington).

[7] ANSI/AISC 360-10. Specification for structural steel buildings. American Institute of Steel Construction (AISC), Chicago, 2010.

[8] D.K. Liu, J. Wardenier, Effect of the yield strength on the static strength of uniplanar K-Joints in RHS (Steel Grade S460, S355 and S235), IIW Doc. XV-E-04-293, 2004.

[9] Y. Kurobane, New Development and Practices in Tubular Joint Design, IIW Doc. XV-448-81 and IIW Doc. XIII-1004-81, 1981.

[10] C. Noordhoek, A. Verheul, R.J. Foeken, H.M. Bolt, P.J. Wicks, Static strength of high strength steel tubular joints, ECSC agreement number 7210-MC/602, 1996.

[11] EN 1993-1-12, Eurocode 3: Design of Steel Structures-Part 1–12: Additional Rules for the Extension of EN 1993 up to Steel Grades S700, European Committee for Standardization, EN 1993-1-12, CEN, Brussels, 2007.

[12] X.L. Zhao, J. Wardenier, J.A. Packer, G.J. van der Vegte, New IIW (2008) static design recommendations for hollow section joints, Tubular Structures XII, CRC Press, Shanghai 2009, pp. 261–269.

[13] J. Becque, T. Wilkinson, The capacity of grade C450 cold-formed rectangular hollow section T and X connections: an experimental investigation, J. Constr. Steel Res. 133 (2017) 345–359.

[14]M. Mohan, T. Wilkinson, FEA of T & X joints in Grade C450 steel, Tubular Structures XIV, CRC Press, London 2012, pp. 185–194.
[15]M. Mohan, T. Wilkinson, Finite element simulations of 450 grade cold-formed K and N joints, Tubular Structures XV, CRC Press, Brazil 2015, pp. 449–456.
[16]S.S. Cheng, J. Becque, A design methodology for sidewall failure of RHS truss X-joints accounting for compressive chord pre-load, Eng. Struct. 126 (2016) 689–702.
[17]R. Puthli, O. Bucak, S. Herion, O. Fleischer, A. Fischl, O. Josat, Adaptation and extension of the valid design formulae for joints made of high-strength steels up to S690 for cold-formed and hot-rolled sections, CIDECT Report 5BT-7/10 (Draft Final Report), CIDECT, Germany, 2011.
[18]C.H. Lee, S.H. Kim, D.H. Chung, D.K. Kim, J.W. Kim, Experimental and numerical study of cold-formed high-strength steel CHS X-joints, J. Struct. Eng. 143 (8) (2017), 04017077.
[19]X.Y. Lan, T.M. Chan, B. Young, Static strength of high strength steel CHS X-joints under axial compression, J. Constr. Steel Res. 138 (2017) 369–379.
[20]Abaqus/Standard. Version 6.13-1. USA: K. a. S. Hibbit; 2013.
[21]L.H. Lu, G.D. de Winkel, Y. Yu, J. Wardenier, Deformation limit for the ultimate strength of hollow section joints, Tubular Structures VI, Balkema, Melbourne 1994, pp. 341–347.
[22]R. Stroetmann, Thoralf Kastner, A. Halsig, P. Mayr, Mechanical properties and a new design approach for welded joints at high strength steels, Engineering Research and Practice for Steel Construction, Hong Kong 2018, pp. 79–90.
[23]F. Javidan, A. Heidarpour, X.L. Zhao, C.R. Hutchinson, J. Minkkinen, Effect of weld on the mechanical properties of high strength and ultra-high strength steel tubes in fabricated hybrid sections, Eng. Struct. 118 (2016) 16–27.
[24]M. Amraei, H. Jiao, X.L. Zhao, L.W. Tong, Fatigue testing of butt-welded high strength square hollow sections strengthened with CFRP, Thin Wall. Struct. 120 (2017) 260–268.
[25]H. Jiao, X.L. Zhao, A. Lau, Hardness and compressive capacity of longitudinally welded very high strength steel tubes, J. Constr. Steel Res. 114 (2015) 405–416.
[26]J. Siltanen, S. Tihinen, J. Kömi, Laser and laser gas-metal-arc hybrid welding of 960 MPa direct-quenched structural steel in a butt joint configuration, J. Laser Appl. 27(S2) (2015) S29007.
[27]M. Amraei, T. Skriko, T. Björk, X.L. Zhao, Plastic strain characteristics of butt-welded ultra-high strength steel (UHSS), Thin Wall. Struct. 109 (2016) 227–241.
[28]J.L. Ma, T.M. Chan, B. Young, Material properties and residual stresses of cold-formed high strength steel hollow sections, J. Constr. Steel Res. 109 (2015) 152–165.
[29]Eurocode 3 (EC3), Design of Steel Structures-Part 1–1: General Rules and Rules for Buildings. European Committee for Standardization, EN 1993-1-1, CEN, Brussels, 2005.
[30]X. Yun, L. Gardner, Stress-strain curves for hot-rolled steels, J. Constr. Steel Res. 133 (2017) 36–46.
[31]J. Wardenier, Hollow Section Joints, Delft University Press, The Netherlands, 1982.
[32]International Institute of Welding (IIW) Subcommission XV-E, XV-701-89: Design recommendations for hollow section joints-predominantly statically loaded, 2nd Ed., 1989 (Helsinki).
[33]G.J. van der Vegte, J. Wardenier, X.L. Zhao, J.A. Packer, Evaluation of new CHS strength formulae to design strengths, Tubular Structures XII, CRC Press, London 2009, pp. 313–322.
[34]D. Pecknold, P. Marshall, J. Bucknell, New API RP2A tubular joint strength design provisions, J. Energ. Resour. 129 (2007) 177–189.
[35]J. Wardenier, Hollow sections in structural applications, 2nd Ed., CIDECT, Geneva, 2011.

[36]G.J. van der Vegte, J. Wardenier, Y. Makino, Effect of chord load on ultimate strength of CHS X-joints, Int. J. Offshore Polar 17 (4) (2007) 301–308.
[37]G.Z. Qiu, J.C. Zhao, Analysis and calculation of axial stiffness of tubular X-joints under compression on braces, J. Shanghai Jiaotong Univ. Sci. 14(4) (2009) 410–417.
[38]J.L. Ma, T.M. Chan, B. Young, Design of cold-formed high strength steel tubular beams, Eng. Struct. 151 (2017) 432–443.
[39]X.Y. Lan, F. Wang, C. Ning, X.F. Xu, X.R. Pan, Z.F. Luo, Strength of internally ring-stiffened tubular DT-joints subjected to brace axial loading, J. Constr. Steel Res. 125 (2016) 88–94.
[40]X.Y. Lan, F. Wang, Z.F. Luo, D.D. Liu, C. Ning, X.F. Xu, Joint strength reduction factor of internally ring-stiffened tubular joints at elevated temperatures, Adv. Struct. Eng. 19(10) (2016) 1650–1660.
[41]W. Li, S. Zhang, W. Huo, Y. Bai, L. Zhu, Axial compression capacity of steel CHS X-joints strengthened with external stiffeners, J. Constr. Steel Res. 141 (2018) 156–166.
[42]H. Nassiraei, L. Zhu, M.A. Lotfollahi-Yaghin, H. Ahmadi, Static capacity of tubular X-joints reinforced with collar plate subjected to brace compression, Thin-Walled Struct. 119 (2017) 256–265.
[43]Y.S. Choo, J.X. Liang, G.J. van der Vegte, J.Y.R. Liew, Static strength of doubler plate reinforced CHS X-joints loaded by in-plane bending, J. Constr. Steel Res. 60 (12) (2004) 1725–1744.
[44]H.T. Li, B. Young, Experimental Investigation of Concrete-Filled High-Strength Steel Tubular X Joints, J. Struct. Eng. 144(10) (2018) 04018178.
[45]H.T. Li, B. Young, Design of concrete-filled high strength steel tubular joints subjected to compression, J. Constr. Steel Res. 150 (2018) 209–220.

Table 1

Effects of heat affected zones on CHS X-joints using S900 and S1100 steel.

Specimen	*d* (mm)	*t* (mm)	d_1 (mm)	t_1 (mm)	*β*	2*γ*	Steel	N_{u1} (kN)	N_{u2} (kN)	N_{u2}/N_{u1}
R69	159.2	9.2	60.6	5.2	0.38	17.3	S900	623	594	0.95
							S1100	657	613	0.93
R69-1	159.2	5.2	60.6	5.2	0.38	30.6	S900	196	188	0.96
							S1100	200	189	0.95
R75	244.7	22.0	194.6	16.0	0.80	11.1	S900	6619	6407	0.97
							S1100	7473	7075	0.95
R75-1	244.7	8.0	194.6	8.0	0.80	30.6	S900	1002	961	0.96
							S1100	1080	1013	0.94

Note: N_{u1} and N_{u2} denote static strengths of CHS X-joints without and with HAZ, respectively.

Table 2

Material parameters adopted for high strength steel.

Steel	E (GPa)	f_y (MPa)	f_u (MPa)	ε_u (%)
S460	210	505	616	10.81
S700	214	772	816	4.64
S900	210	1054	1116	2.26
S900-R10	210	949	1004	2.26
S900-R20	210	843	893	4.75
S1100	207	1152	1317	2.20
S1100-R15	207	979	1119	2.20
S1100-R30	207	806	922	7.70

Note: The value following the letter R denotes the percentage of strength reduction compared with the base metals of S900 and S1100 steel.

Table 3

Comparison of CIDECT mean strengths with test strengths for CHS X-joints without chord preload.

Specimen	β	2γ	Steel	f_y (MPa)	f_u (MPa)	N_{Test} (kN)	$N_{CIDECT,Mean}/N_{Test}$	$N_{Proposed,Mean}/N_{Test}$
R45 [17]	1.00	22.3	S460	485	659	1016	0.92	0.88
R60 [17]	0.44	31.5	S460	535	587	781	1.13	1.06
R61 [17]	0.39	31.3	S460	535	587	725	1.14	1.07
R62 [17]	0.57	22.0	S460	485	659	374	1.01	0.97
R73 [17]	0.81	26.5	S460	486	589	544	1.20	1.15
R32 [17]	0.55	21.9	S690	734	802	1774	1.03	0.91
R33 [17]	0.55	17.0	S690	739	798	2531	1.17	1.03
R42 [17]	1.00	21.5	S690	727	793	1399	1.07	0.95
R68 [17]	0.62	17.2	S770	904	946	314	1.26	1.05
R69 [17]	0.38	17.3	S770	858	879	519	1.15	0.97
R70 [17]	0.77	15.2	S770	847	892	968	1.23	1.05
R71 [17]	0.72	19.2	S770	854	900	1095	1.23	1.04
R72 [17]	0.53	18.9	S770	894	937	1868	1.29	1.08
R74 [17]	0.65	11.1	S770	811	863	4143	1.17	1.01
R75 [17]	0.80	11.1	S770	811	863	5298	1.23	1.06
X90-650-0.75-16 [18]	0.75	16.0	HSA800	764	905	6965	1.09	0.95
X90-650-0.62-26 [18]	0.62	26.0	HSA800	798	914	5612	1.17	1.01
Mean							1.15	1.01
COV							0.080	0.067

Note: The nominal yield stress and ultimate stress of HSA800 steel are 650 and 800 MPa, respectively.

Table 4

Results of statistical analysis for CHS X-joints without chord preload.

Steel	$N_{\mathrm{CIDECT,Mean}}/N_{\mathrm{FE}}$			$N_{\mathrm{Proposed,Mean}}/N_{\mathrm{FE}}$		
	No. of data	Mean	COV	No. of data	Mean	COV
S460	81	1.01	0.073	63	0.97	0.065
S700	81	1.17	0.085	63	1.02	0.074
S900	81	1.35	0.128	45	1.01	0.085
S1100	81	1.40	0.156	45	0.98	0.107
Total	324	1.23	0.175	216	0.99	0.084

Table 5

Results of statistical analysis for CHS X-joints subjected to chord preload.

Steel	$Q_{f,CIDECT}/Q_{f,FE}$			$Q_{f,Proposed}/Q_{f,FE}$		
	No. of data	Mean	COV	No. of data	Mean	COV
S460	96	0.93	0.059	96	0.96	0.052
S700	96	0.91	0.056	96	0.99	0.059
S900	96	0.89	0.065	64	0.99	0.043
S1100	96	0.88	0.076	64	0.98	0.036
Total	384	0.90	0.067	320	0.98	0.051

Table 6

Results of statistical analysis for CHS X-joints without and with chord preload.

Steel	$N_{CIDECT,Mean}/N_{FE}$			$N_{Proposed,Mean}/N_{FE}$		
	No. of data	Mean	COV	No. of data	Mean	COV
S460	165	1.03	0.150	147	1.01	0.163
S700	165	1.10	0.111	147	0.99	0.092
S900	165	1.26	0.149	101	0.98	0.098
S1100	165	1.29	0.177	101	0.94	0.118
Total	660	1.17	0.176	496	0.98	0.126

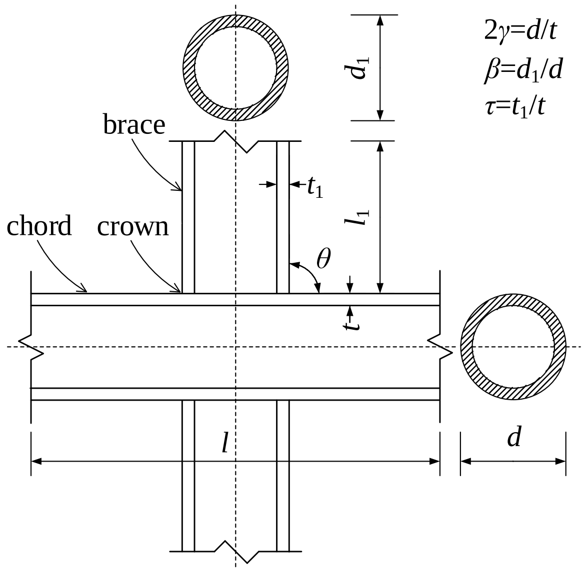

Fig. 1. Configuration and notations of CHS X-joints.

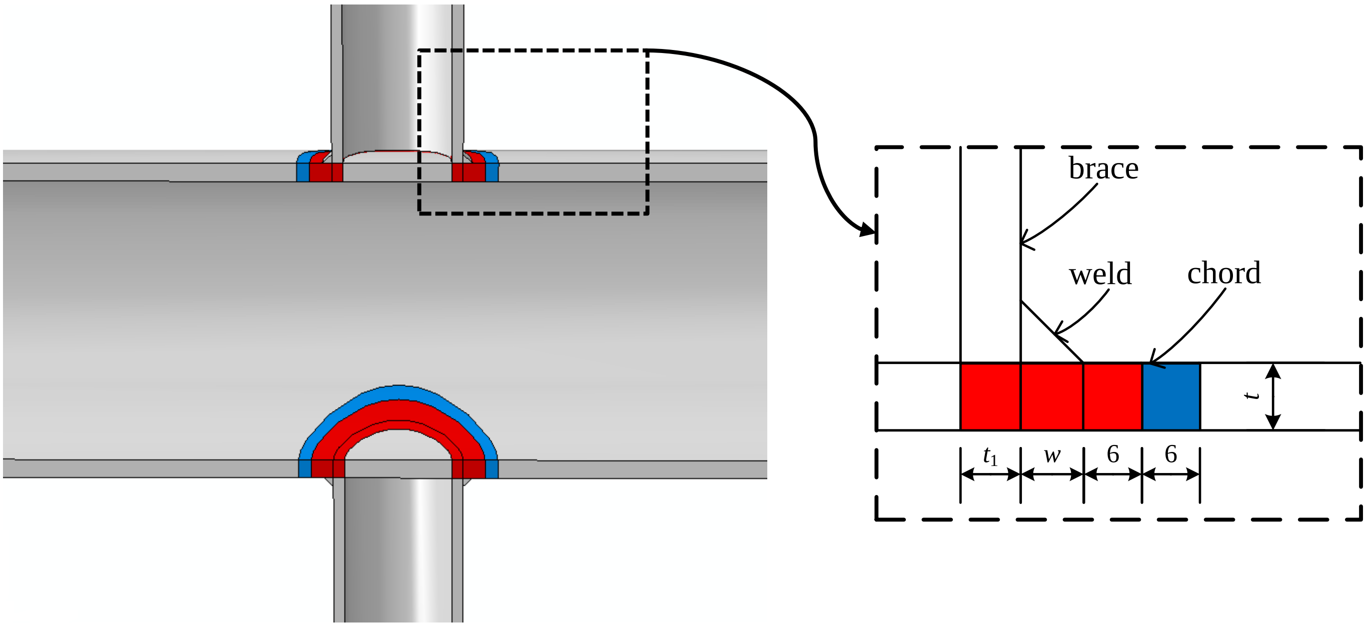

Fig. 2. Heat affected zones in CHS X-joints (dimensions in mm).

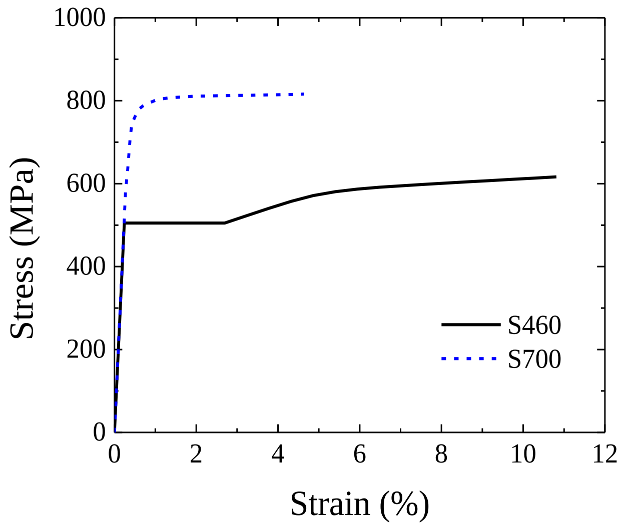

(a) S460 and S700

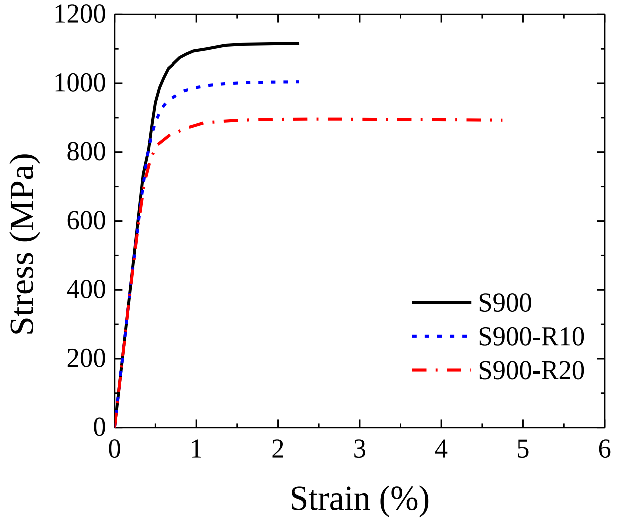

(b) S900

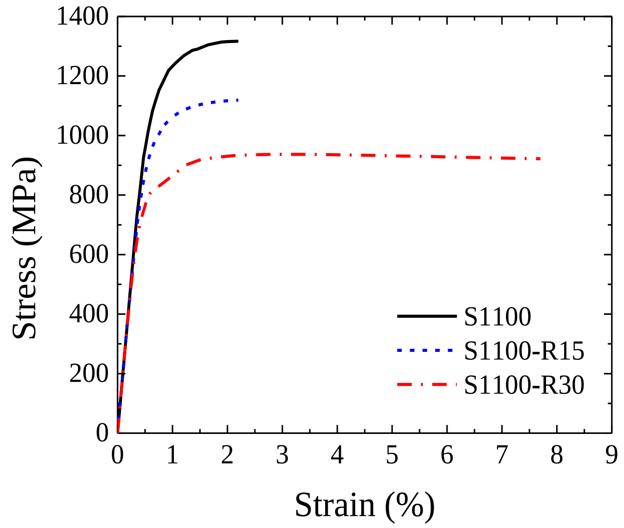

(c) S1100

Fig. 3. Engineering stress-strain curves of high strength steel.

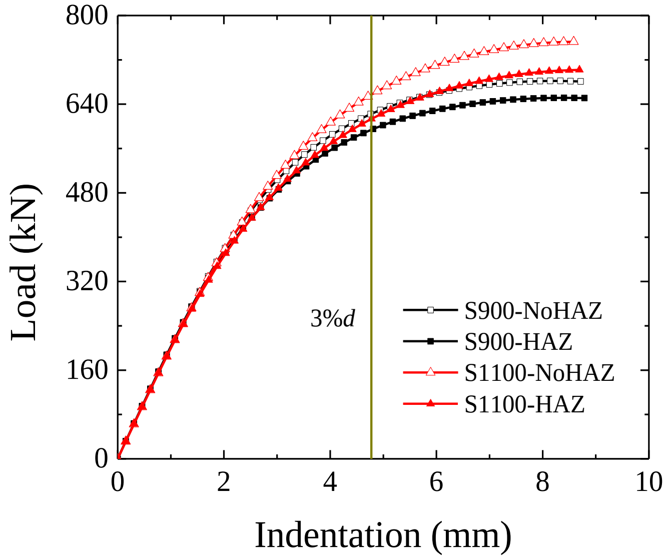

(a) R69

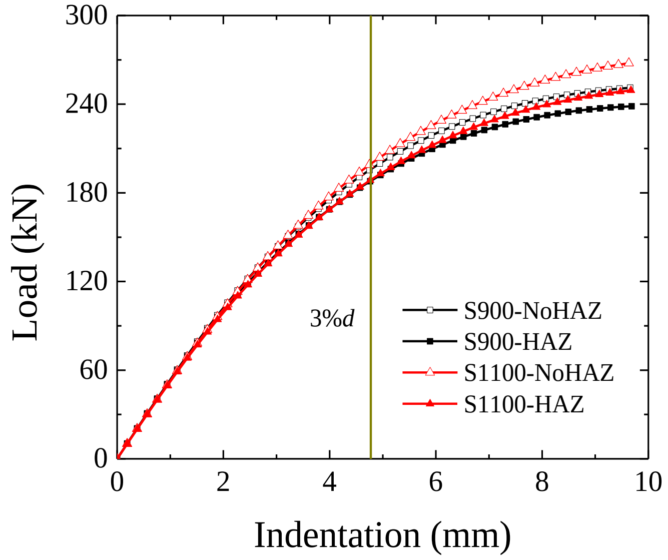

(b) R69-1

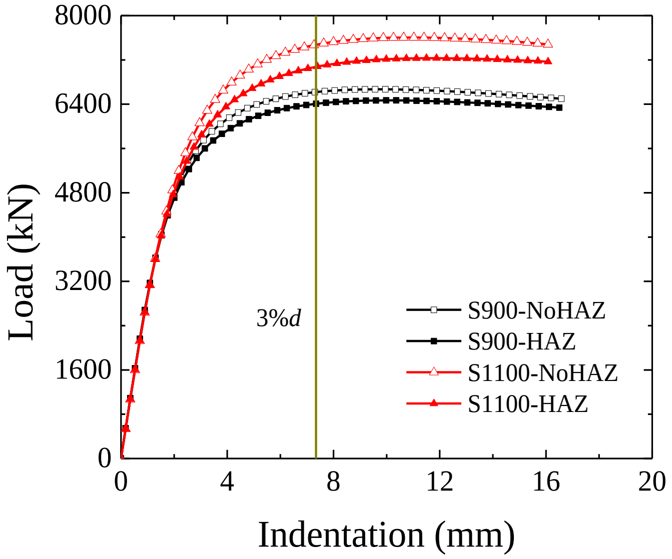

(c) R75

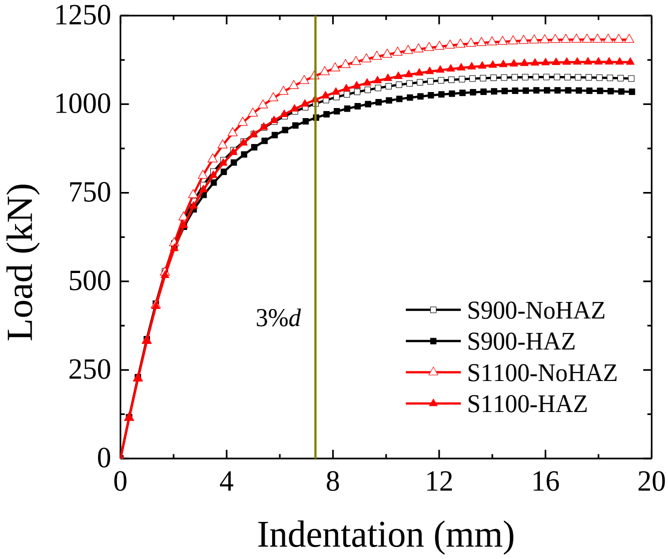

(d) R75-1

Fig. 4. Effects of heat affected zones on CHS X-joints using S900 and S1100 steel.

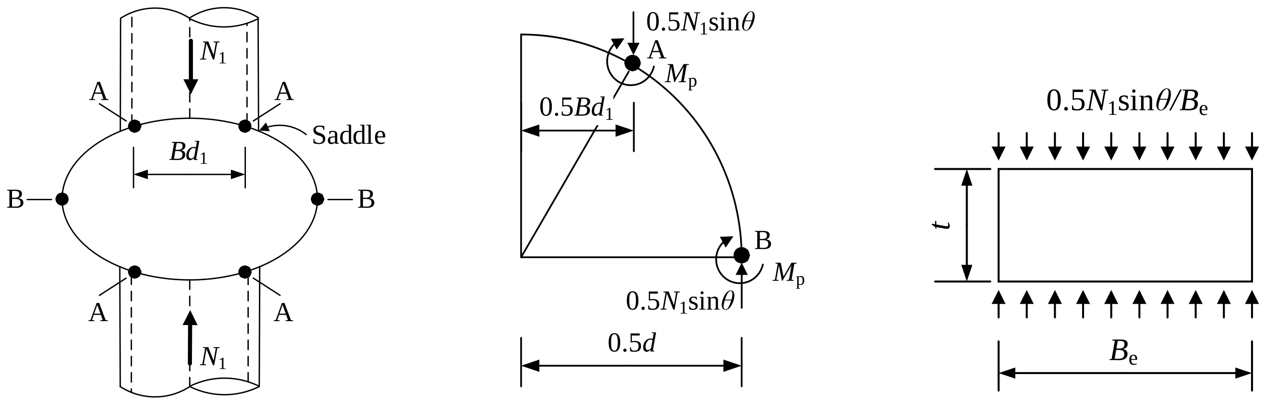

(a) Assumed location of plastic hinges (b) A fourth model (c) Plastic hinge (along the chord)

Fig. 5. Ring model for CHS X-joints using normal strength steel.

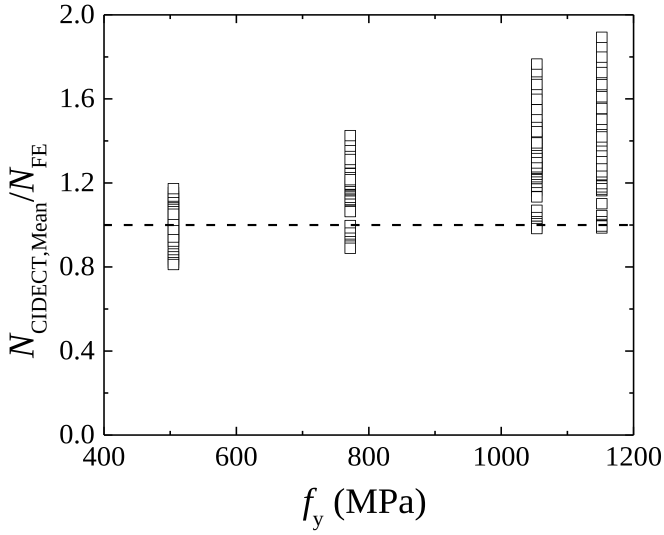

(a) Numerical simulations

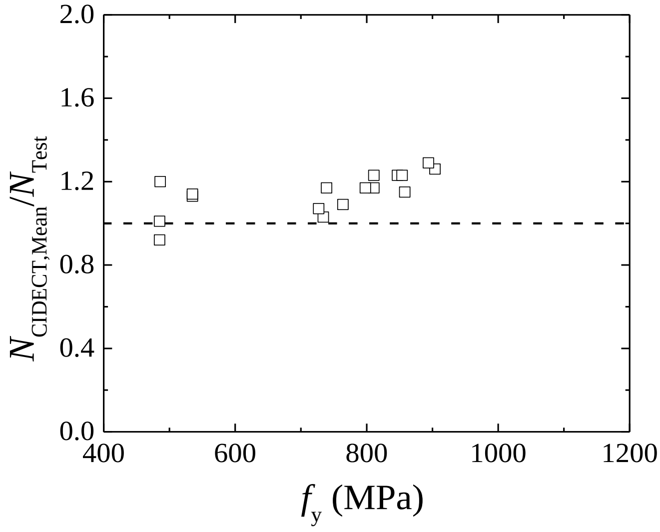

(b) Experimental tests

Fig. 6. Comparison of CIDECT mean strengths with numerical and test strengths of CHS X-joints without chord preload.

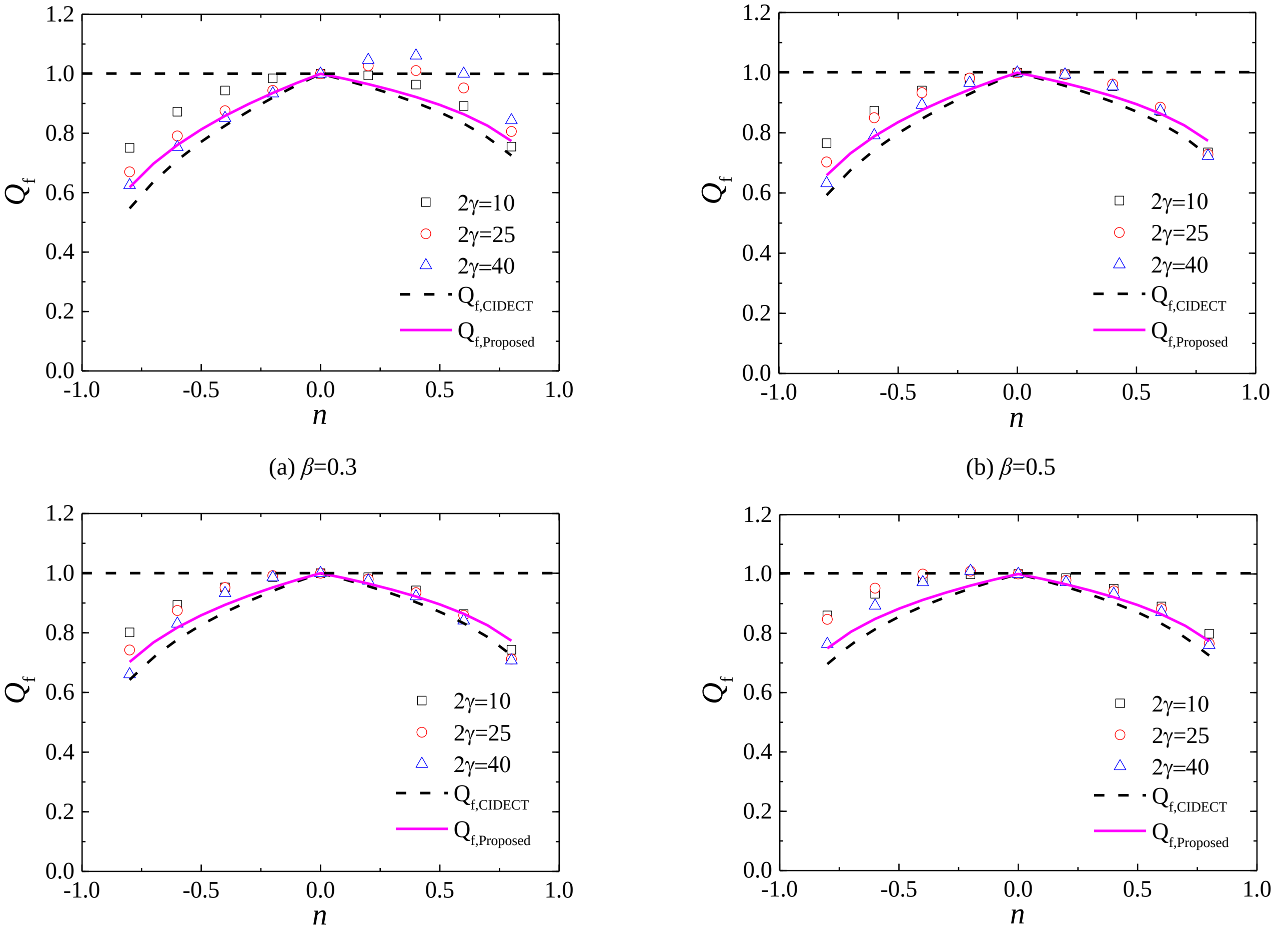

(a) β=0.3 (b) β=0.5

(c) β=0.7 (d) β=0.9

Fig. 7. Comparison of joint strength reduction for S460 CHS X-joints under chord preload.

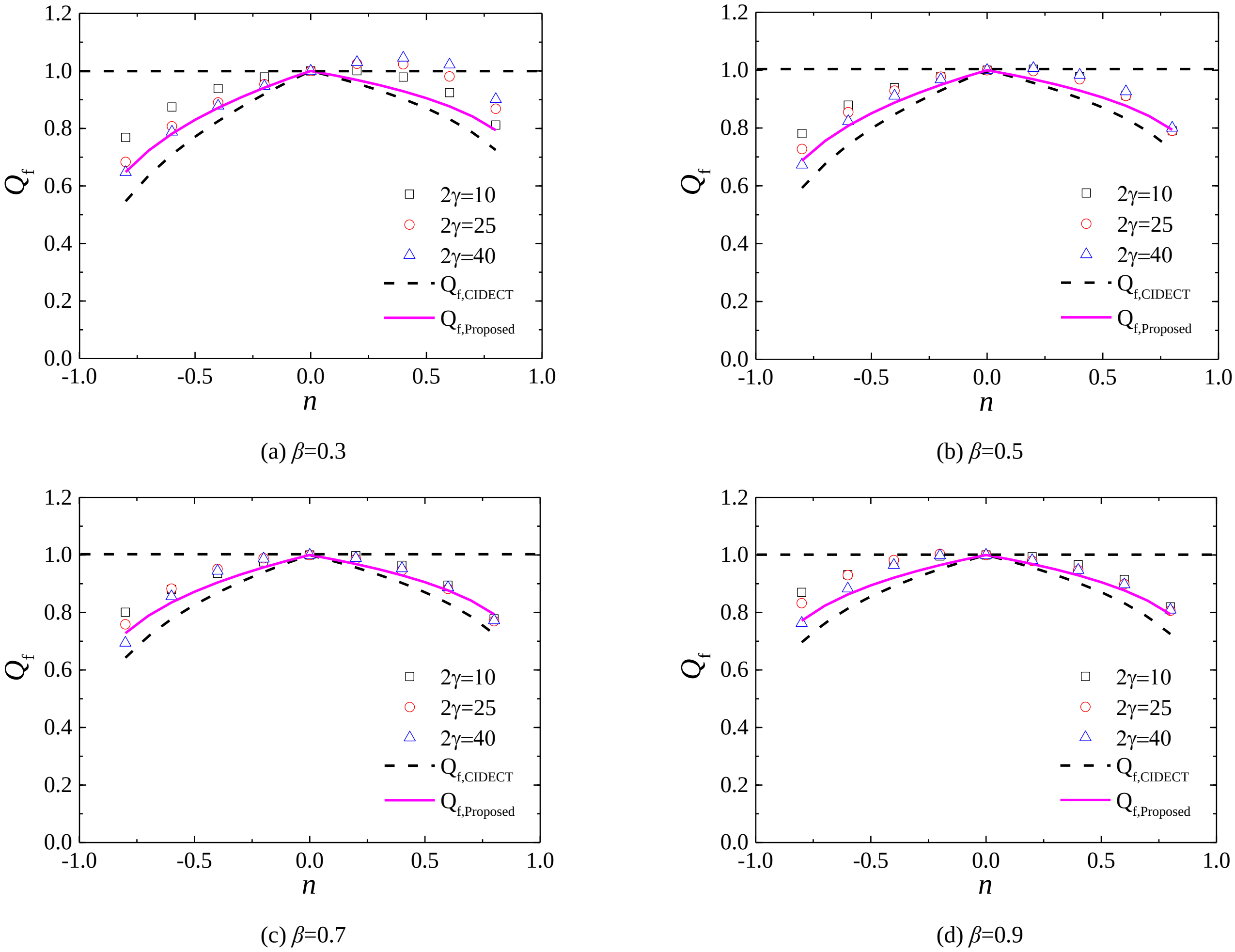

Fig. 8. Comparison of joint strength reduction for S700 CHS X-joints under chord preload.

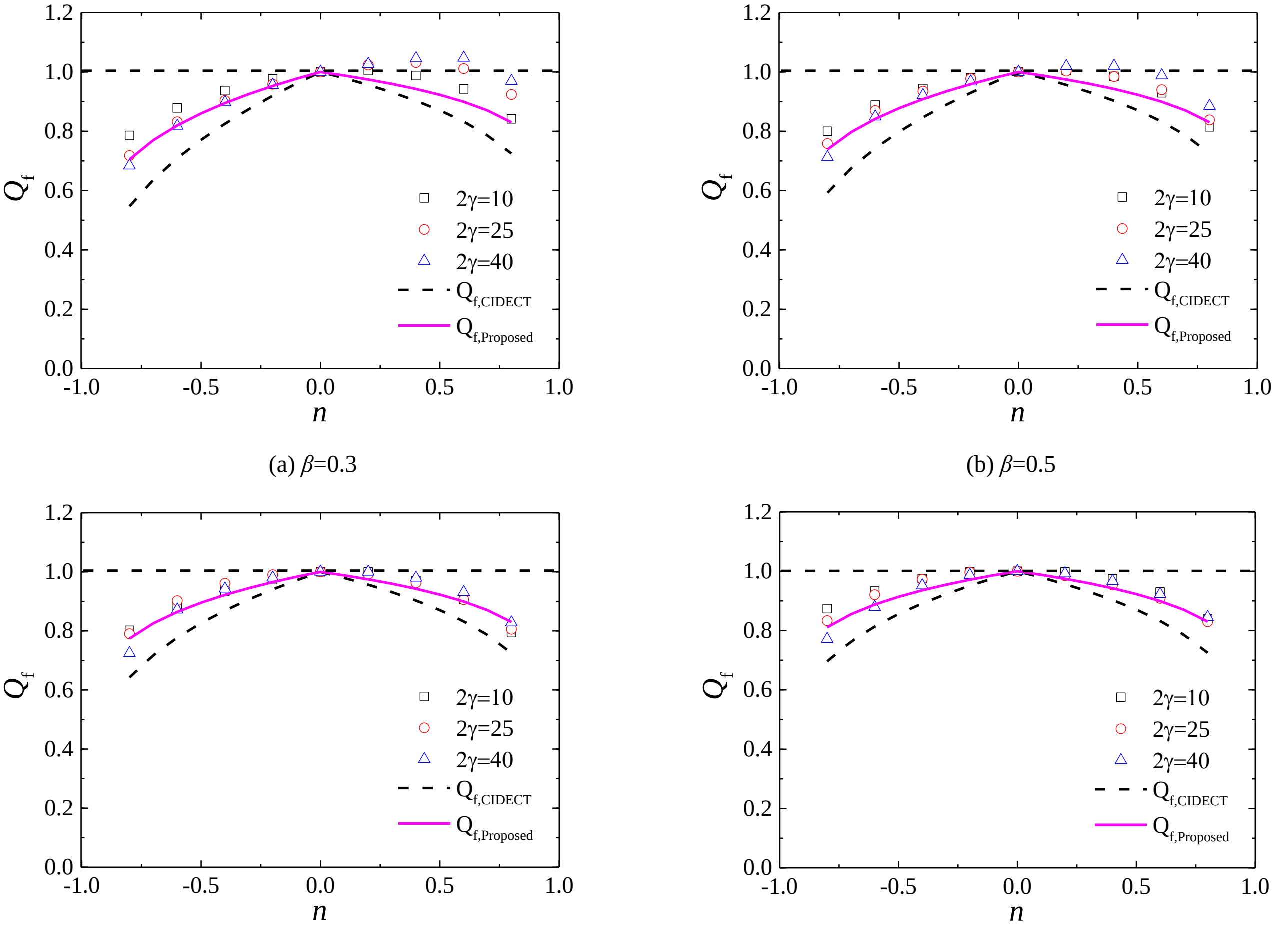

(a) β=0.3

(b) β=0.5

(c) β=0.7

(d) β=0.9

Fig. 9. Comparison of joint strength reduction for S900 CHS X-joints under chord preload.

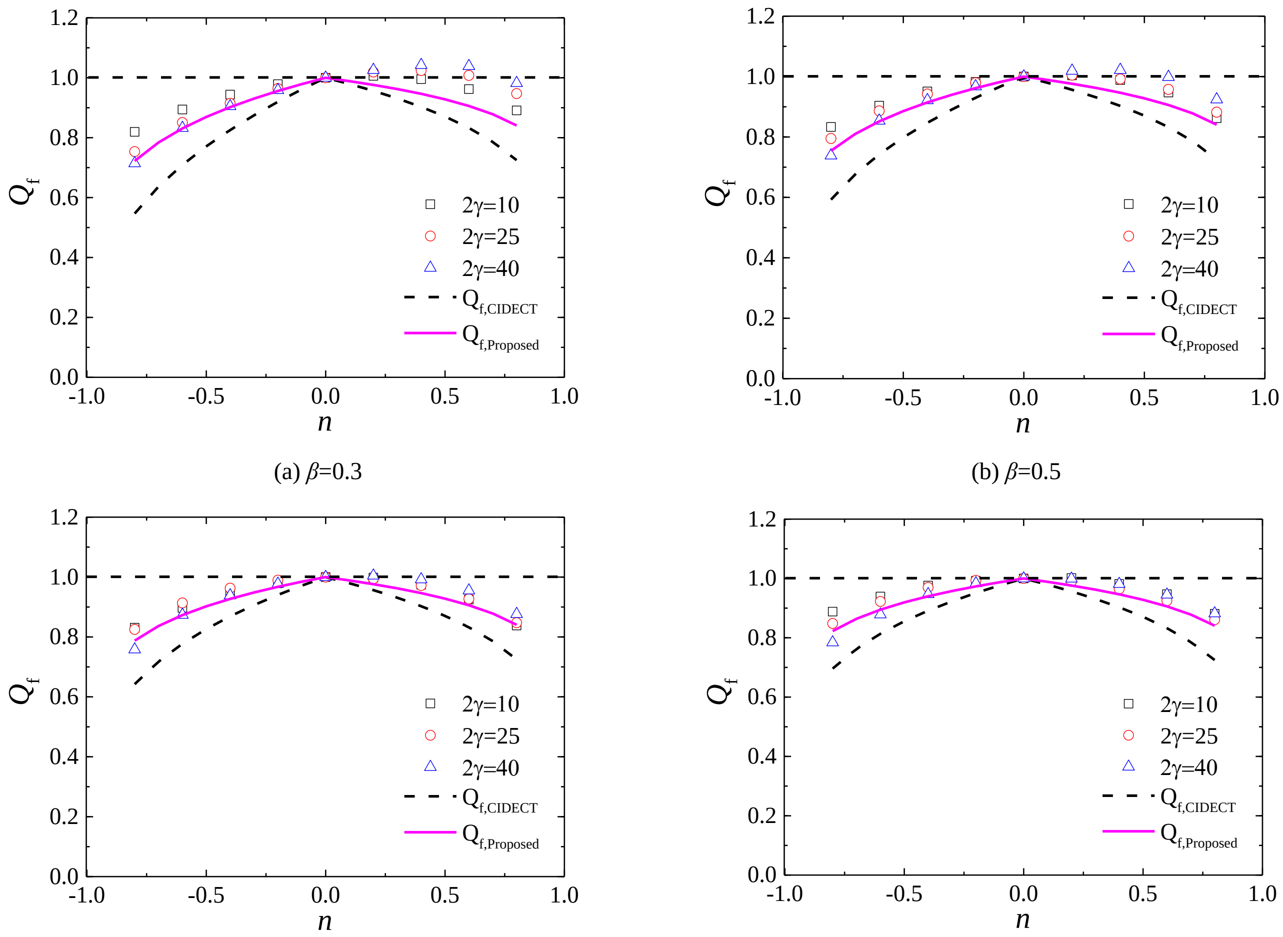

(a) β=0.3 (b) β=0.5

(c) β=0.7 (d) β=0.9

Fig. 10. Comparison of joint strength reduction for S1100 CHS X-joints under chord preload.

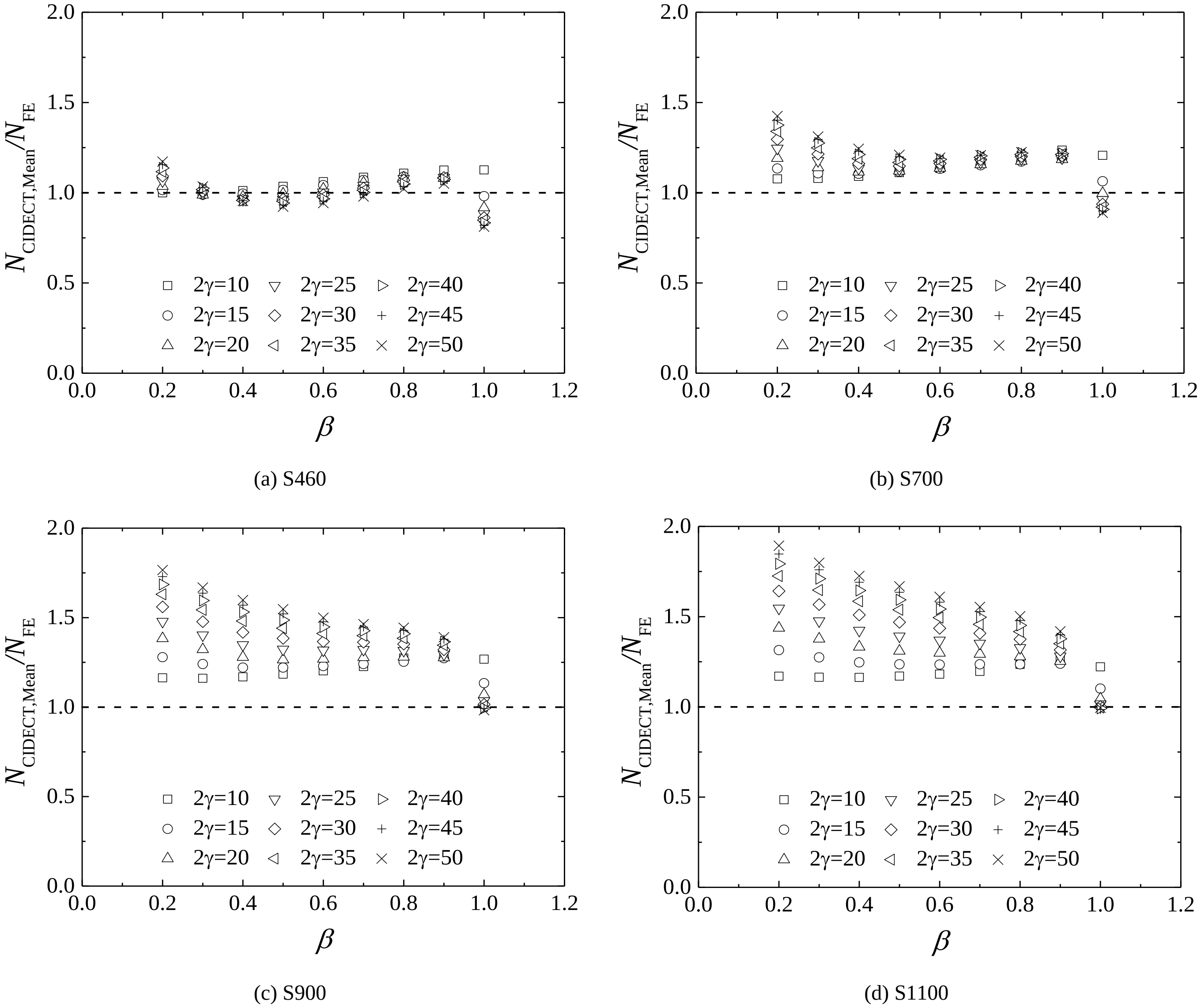

Fig. 11. Effects of β and 2γ ratios on $N_{CIDECT,\ Mean}/N_{FE}$ ratio of CHS X-joints without chord preload.

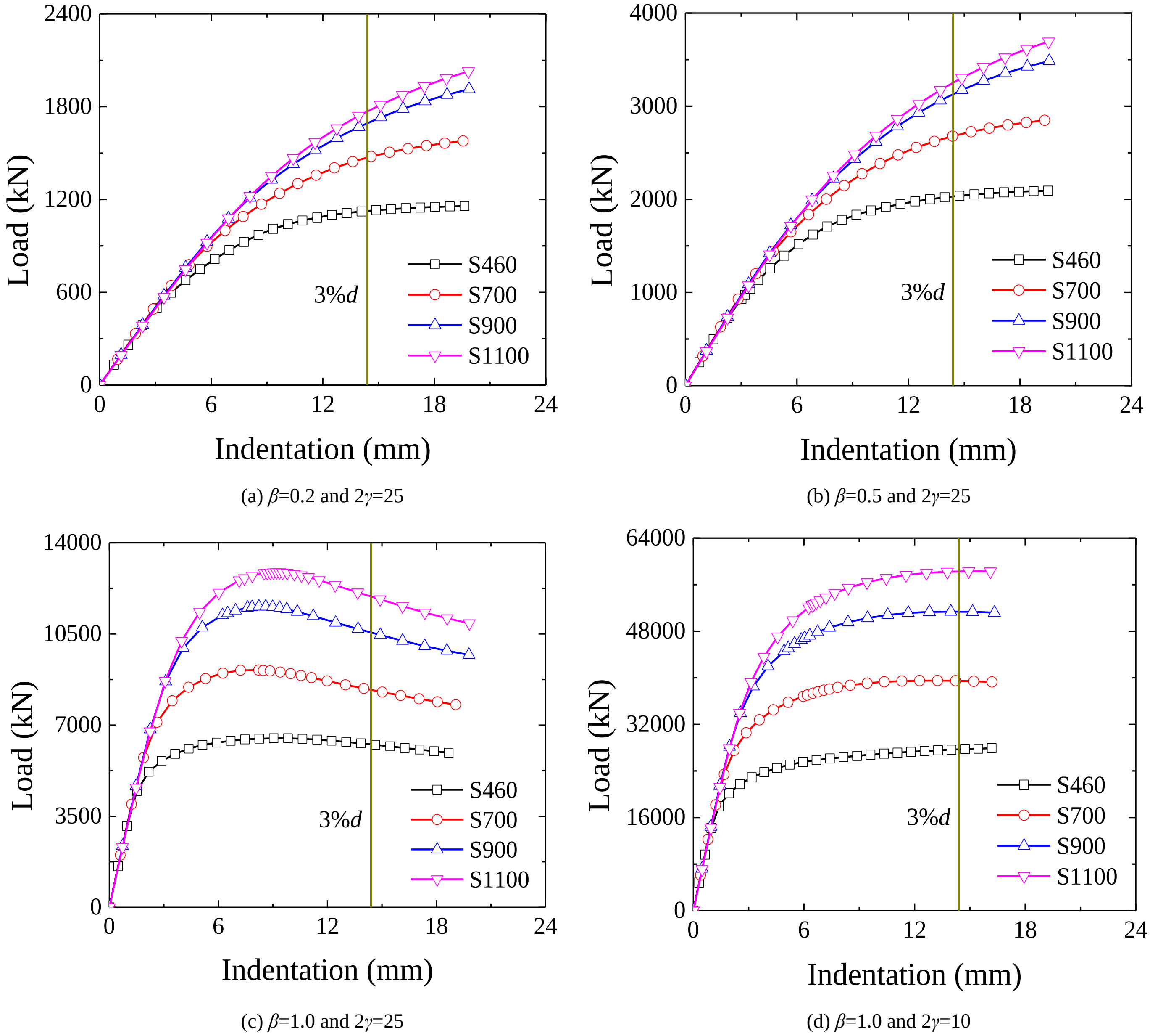

(a) β=0.2 and 2γ=25

(b) β=0.5 and 2γ=25

(c) β=1.0 and 2γ=25

(d) β=1.0 and 2γ=10

Fig. 12. Typical load-indentation curves of CHS X-joints without chord preload.

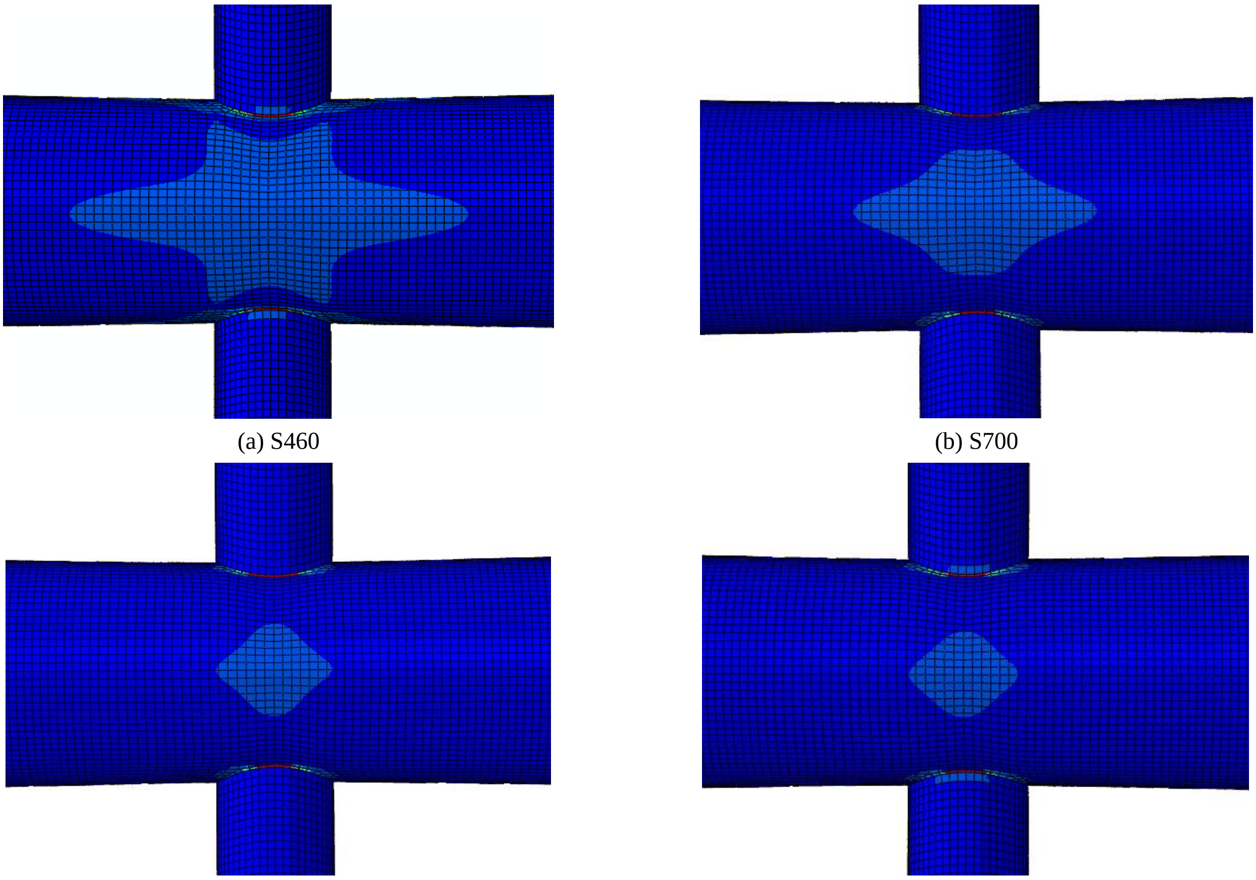

(a) S460 (b) S700

(c) S900 (d) S1100

Fig. 13. Typical yielding patterns of CHS X-joints with β=0.5 and 2γ=25.